



MJ233X HT24 Degree Project in Heat and Power Technology
Second Cycle, 30.0 credits

A comprehensive optimization tool for PV-BESS co-location for trading in the market

Alexis BLUMENAU



Master of Science Thesis
Department of Energy Technology
KTH 2025

**A comprehensive optimization tool for
PV-BESS co-location for trading in the
market**

TRITA-ITM-EX 2025:40

Alexis Blumenau

Approved:

Examiner

Supervisor

Jagruti Thakur

Jagruti Thakur

Date of grading:

Industrial Supervisor

Contact person

Christian Schelander
(Flower AB)

Jagruti Thakur

Abstract

The transition to renewable energy sources has increased the demand for flexible and efficient energy storage solutions to address the *variability of power generation*. *This master's thesis* focuses on the development of an optimization tool to determine the optimal sizing of a Battery Energy Storage System (BESS) co-located with a photovoltaic (PV) power plant. The tool is designed to support financial and technical decision-making by evaluating the viability of hybrid projects under different operational and market conditions. The work has then been applied to a 10 MW PV system in Hallstahammar, Sweden.

Key functionalities of the tool include solar power generation forecasting, an initial price prediction model for electricity wholesale markets, and the integration of the BESS into frequency regulation markets, particularly FCR-D (Frequency Containment Reserve for Disturbances). Additionally, the tool incorporates a battery degradation model to assess the long-term impact of various operating strategies on the system's economic performance. Arbitrage operations lead to 36.2% capacity fading, while FCR-D participation results in a lower degradation rate around 11.5% primarily due to calendar aging rather than deep cycling.

By simulating multiple scenarios and considering regulatory, market, and technological constraints, the tool provides insights into optimal system configurations that maximize revenues from market participation while minimizing degradation-related costs. The proposed approach enables stakeholders to make informed decisions regarding the implementation of co-located PV-BESS projects, contributing to the decarbonization of energy systems and enhancing grid stability. The results indicate that arbitrage is not a viable strategy under current market conditions, yielding a negative Net Present Value (NPV) across all scenarios. Conversely, FCR-D participation offers a significantly more favorable economic outcome, with optimal BESS sizes of 41 MW, *generating an NPV of up to €1.78 million. Furthermore, in Scenario 3, leveraging excess PV generation contributes an additional €1.08 million in revenue.*

This study demonstrates the potential of co-location projects to improve the integration of renewable energy into the grid while ensuring the profitability and reliability of energy storage investments. The findings underscore the importance of market selection, as FCR-D participation provides stable revenue streams and justifies larger BESS capacities, while arbitrage alone remains unprofitable.

Key Words:

Battery Energy Storage System, Co-location, Photovoltaic power plant, Optimization tool, Ancillary services, Arbitrage, Grid Scale

Sammanfattning

Övergången till förnybara energikällor har ökat efterfrågan på flexibla och effektiva energilagringssystem för att hantera variabiliteten i kraftproduktionen. Denna masteruppsats fokuserar på utvecklingen av ett optimeringsverktyg för att bestämma den optimala dimensioneringen av ett batterilagringssystem (BESS) som är samlokaliserat med ett solcellskraftverk (PV). Verktöget är utformat för att stödja ekonomiskt och tekniskt beslutsfattande genom att utvärdera lönsamheten för hybridprojekt under olika drifts- och marknadsförhållanden. Arbetet har tillämpats på ett 10 MW PV-system i Hallstahammar, Sverige.

Verktögets nyckelfunktioner omfattar prognoser för solkraftsproduktion, en modell för att förutsäga det initiala priset på grossistmarknaderna för el och integrationen av BESS på marknaderna för frekvensreglering, särskilt FCR-D (Frequency Containment Reserve for Disturbances). Dessutom innehåller verktöget en batteridegraderingsmodell för att bedöma den långsiktiga effekten av olika driftstrategier på systemets ekonomiska prestanda. Arbitrageoperationer leder till 36,2% kapacitetsförlust, medan FCR-D-deltagande resulterar i en lägre degraderingsgrad på cirka 11,5%, främst på grund av kalenderåldrande snarare än djupcykling.

Genom att simulera flera scenarier och ta hänsyn till regleringar, marknad och tekniska begränsningar ger verktöget insikter i optimala systemkonfigurationer som maximerar intäkterna från marknadsdeltagande samtidigt som degraderingsrelaterade kostnader minimeras. Det föreslagna tillvägagångssättet gör det möjligt för intressenter att fatta välgrundade beslut om genomförandet av samlokaliserade PV-BESS-projekt, vilket bidrar till att minska koldioxidutsläppen i energisystemen och förbättra nätstabiliteten. Resultaten visar att arbitrage inte är en hållbar strategi under rådande marknadsförhållanden, utan ger ett negativt nettonuvärde (NPV) i alla scenarier. Omvänt ger FCR-D-deltagande ett betydligt mer gynnsamt ekonomiskt utfall, med optimala BESS-storlekar på 41 MW, vilket genererar ett NPV på upp till 1,78 miljoner euro. I Scenario 3 bidrar dessutom överskottsproduktion av solceller med ytterligare 1,08 miljoner euro i intäkter.

Den här studien visar att samlokaliseringsprojekt kan förbättra integrationen av förnybar energi i elnätet och samtidigt säkerställa lönsamheten och tillförlitligheten för investeringar i energilagring. Resultaten understryker vikten av marknadsval, eftersom FCR-D-deltagande ger stabila intäktsströmmar och motiverar större BESS-kapacitet, medan enbart arbitrage förblir olönsamt.

Acknowledgments

First, I would like to thank Christian Schelander for his guidance in this work and tool development, giving helpful insights on the interesting aspects to cover from an asset development point of view. I want to thank Jan Dautel for his technical guidance on the topic and on the Python environment.

A thought goes to the whole Asset development domain at FLOWER who made this thesis journey really enjoyable, and a special thanks to the BeNeFr squad and France team, all of whom provided a very pleasant daily work environment.

Finally, I thank my academic supervisor, Jagruti Thakur, for her guidance and advice throughout this project work.

Contents

Abstract.....	3
Sammanfattning.....	4
Acknowledgments.....	5
List of abbreviations.....	7
List of tables.....	7
List of figures.....	8
1. Introduction.....	9
2. Literature Review.....	11
3. Scope and Research questions.....	19
4. Methodology.....	20
4.1. Overview of the tool.....	20
4.2. Inputs and pre-calculations.....	24
4.3. Dual-loop optimization.....	39
4.4 Case study.....	47
5. Results.....	51
5.1. Arbitrage on the spot market.....	51
5.2. FCR-D participation.....	56
5.3. Summary of results.....	59
6. Limitations and future work.....	62
Limitations.....	62
Unaddressed aspects.....	62
Future work.....	63
7. Sustainability assessment.....	64
8. Conclusion.....	66
9. References.....	67

List of abbreviations

BESS	Battery Energy Storage System
PV	Solar Photovoltaic
FCR-D	Frequency Containment Reserve for Disturbances
ESS	Energy Storage System
CAPEX	Capital Expenditure
OPEX	Operational Expenditure
AC / DC	Alternative Current / Direct Current
NPV	Net Present Value
IRR	Internal rate of return
WACC	Weighted Average Cost of Capital
TMY	Typical Meteorological Year
TSO	Transmission System Operator
DSO	Distribution System Operator
SoC	State of Charge
DoD	Depth of Discharge

List of tables

Table 1: Inputs and outputs of the tool	22
Table 2: Evolution of irradiation and temperature towards 2039 and 2050 [42] [50]	25
Table 3: Standard PV module specifications [51]	26
Table 4: Input parameters for the arbitrage optimization problem.....	40
Table 5: Variables for the arbitrage optimization problem.....	41
Table 6: Variables for the FCR-D participation optimization problem.....	42
Table 7: Constant parameters for degradation costs linearization	45
Table 8: Input data related to the chosen case study [59][60].....	48
Table 9: Grid capacity in both directions for the PV plant and the BESS under each scenario	51
Table 10: Results for all configurations (2 markets, 3 scenarios).....	59

List of figures

Fig 1: Global power system flexibility needs and supply, 2022-2050 (reworked from [4])	10
Fig 2: Optimization based on the cost-efficiency of a micro-grid [16].....	12
Fig 3: Methodology of the tool.....	21
Fig 4: PV generation forecasts methodology.....	24
Fig 5: PV module electrical equivalent circuit [55]	27
Fig 6: FCR-D activation as a function of the frequency.....	32
Fig 7: Flowchart of the price forecasting model	32
Fig 8 (a)(b): Price phasing over a year (a) and a day (b) for Sweden	33
Fig 9: AC-coupled grid connection of PV plant and BESS.....	34
Fig 10: Grid connection capacity repartition between PV and BESS in scenario 1	35
Fig 11(a)(b): usable BESS capacity under scenario 1 for a 1.5MW BESS (a) and 2.5MW BESS (b).....	36
Fig 12: Grid connection capacity repartition between PV and BESS in scenario 2	37
Fig 13: Usable capacity for the BESS over time in scenario 2	37
Fig 14: Example of inverter clipping on a summer day for a 8MW PV plant and a DC/AC ratio of 1.5.....	38
Fig 15: Block diagram of the dual-stage optimization	39
Fig 16: PV generation profiles on a winter and a summer day.....	49
Fig 17: Long-term price trends for Spot market, FCR-D Up and Down.....	49
Fig 18: NPV per battery capacity - Spot Market - Scenario 1.....	52
Fig 19: Income per battery capacity - Spot Market - Scenario 1	52
Fig 20: NPV per battery capacity - Spot Market - Scenario 2.....	53
Fig 21: Income per battery capacity - Spot Market - Scenario 2	54
Fig 22: NPV per battery capacity - Spot Market - Scenario 3.....	54
Fig 23: Comparison of incomes per battery capacity - Spot Market - Scenarios 2 and 3	55
Fig 24: Degradation over lifetime for arbitrage in scenarios 1, 2 and 3 for a 35 MW battery	55
Fig 25: NPV per battery capacity - FCR-D - Scenario 1.....	57
Fig 26 (a)(b): NPV per battery capacity - FCR-D - Scenario 2: Complete range (a) and Zoom (b)	57
Fig 27 (a)(b): NPV per battery capacity - FCR-D - Scenario 3 (a) and Scenario 2-3 comparison (b).....	58
Fig 28: Degradation over lifetime for FCR-D in scenarios 1, 2 and 3 for a 35 MW battery ...	58

1. Introduction

Europe's electricity sector is undergoing radical change, driven by ambitious decarbonization targets and the growing integration of renewable energies. The European Union's energy strategies, stated in the European Green Deal adopted in 2020, aim to achieve carbon neutrality by 2050, with an intermediate stage of reducing by 55% by 2030 compared to 1990 levels, requiring a significant reduction in greenhouse gas emissions [1]. These targets imply a substantial increase in the share of renewable energy sources in the energy mix. The International Energy Agency (IEA) estimates that the global installed renewable energy capacity should be triple by 2030 [2].

Among renewable energy sources, solar photovoltaic (PV) stands out due to its ability to generate clean and abundant energy. Over the past decade, PV has transformed the energy landscape with costs dropping tenfold [3]. According to the IEA, achieving the renewable energy targets for 2030 and 2050 relies heavily on a significant growth in PV capacity, which is projected to exceed 8,500 GW by 2050. This would position PV as the dominant source in the electricity mix, accounting for approximately 40% of the total share [3]. However, the variability of renewable energy sources presents substantial challenges for maintaining power grid stability.

To meet these challenges, battery energy storage systems (BESS) are emerging as essential solutions. BESS has indeed proven to be able to manage this issue by responding quickly to frequency deviations by injecting or absorbing power from the grid. The implementation of BESS on electricity grids has skyrocketed over the past years, starting from less than 5 GW in 2017 and reaching 83GW cumulative installed capacity in 2023 [4]. And this fast development is expected to accelerate even more, thanks to long-term plans and cost decrease. During the last Conference of Parties COP29 in Baku, Azerbaijan, the Global Energy Storage and Grids Pledge committed to a new target of 1,500 GW installed Energy Storage Systems (ESS) capacity by 2030 [4], 80% of which would be BESS [5]. An ambitious goal that will be pursued with the help of policies that will make the implementation faster.

This acceleration is also accompanied by a large drop in components prices, cutting in half over the past 5 years, down to about 100\$/MWh [6]. In parallel, as Europe becomes a major player in the BESS scene with about 15% of newly installed capacity [7], the EU launched in 2017 the European Battery Alliance (EBA). The goal of this alliance is to ensure a stable, competitive and sustainable battery cell manufacturing value chain in Europe [8] helping keep component prices stable in the future as they might face peaks due to lithium scarcity [9]. Both these parameters, and additional ones such as the expansion of recycling and second-life supply chains, will help even further develop the use of BESS for grid-scale stationary cases.

To tackle the increase of renewables and the need for grid stability, new advanced configurations emerge, combining different energy systems to take advantage of all technologies, while limiting their downsides [10]. The most common example is the combination of a PV power plant with a battery storage system. The IEA indeed estimates that solar PV will be the main flexibility needs driver by 2050, whereas BESS will be the main flexibility supplier, as seen in Fig 1 [4].

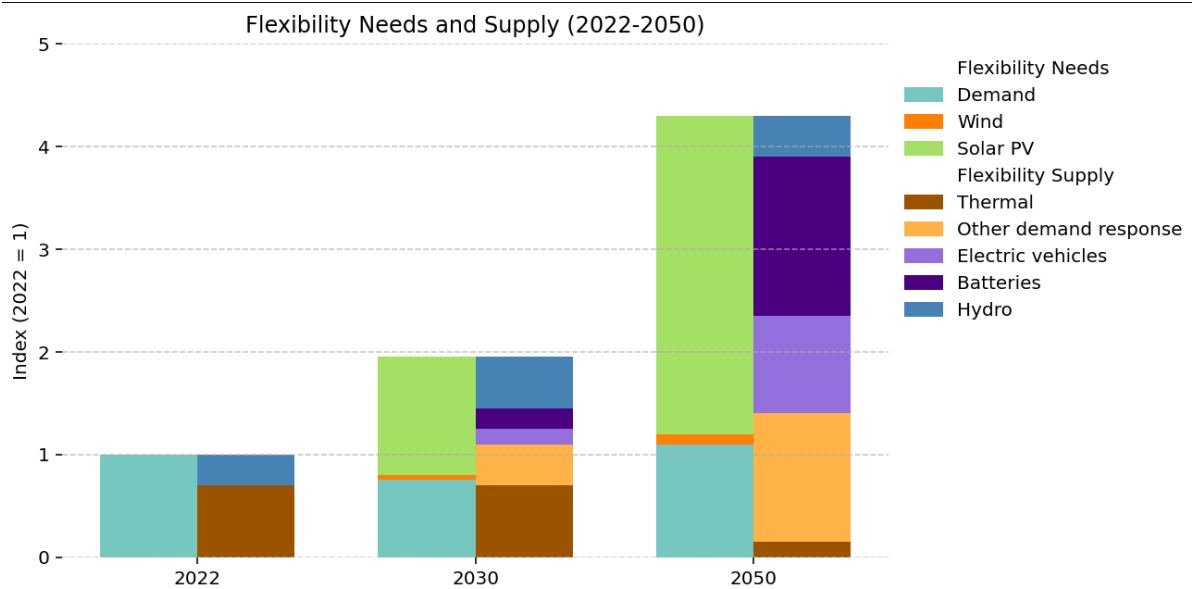


Fig 1: Global power system flexibility needs and supply, 2022-2050 (reworked from [4])

Therefore, this kind of co-location offers strategic and economic opportunities. By pooling infrastructures such as land and grid connection points, co-location will help reduce installation costs by up to 40% by 2030 while increasing operational flexibility and will make PV-BESS co-located one of the most competitive energy sources [4]. Moreover, this approach makes better use of local resources and maximizes the value of the energy produced, by e.g. benefiting from the curtailed PV energy. About 1.9 TWh of solar generated energy was curtailed in 2022 in California (the equivalent of powering 200,000 homes for an entire year), and part of it, if not all, could have been stored with the help of a BESS [11].

Not only can co-located PV-BESS projects help increase renewable share on the grid but also help to build a resilient grid through participation in frequency balancing markets. By providing grid support services, BESS operators can leverage their storage capacity to help balance the grid, mitigate frequency fluctuation, and ensure system reliability. This not only contributes to the overall stability and resilience of the electricity grid but also enhances the value of BESS [12]. These markets, which remunerate players capable of providing rapid reserves in the event of fluctuations in grid frequency, represent a major economic opportunity for BESS.

In this context, the development of tools for optimizing the design and management of co-located energy systems is essential. These tools can be used to simulate different operating scenarios, estimate battery degradation costs, and maximize revenues from wholesale and balancing markets. This thesis is part of this approach, proposing an innovative solution to help decision-makers assess the profitability of PV-BESS projects, while contributing to the acceleration of the energy transition.

2. Literature Review

The deployment of Battery Energy Storage Systems (BESS) is expanding at an exponential rate. This growth is driven not only by decreasing costs but also by the increasing number of potential applications, which in turn heightens the demand for large-scale BESS.

One of the most common uses of BESS is energy arbitrage. In reference [13], arbitrage is *defined as “the application of energy trading strategies within an electricity market environment, aiming to buy energy from the grid at a low price and sell it back at a significantly higher price, thereby capitalizing on spot market price fluctuations.”* This strategy can be combined with other applications, such as providing ancillary services.

Several studies explore potential synergies and revenue stacking when simultaneously delivering an ancillary service (specifically Enhanced Frequency Response) and engaging in arbitrage e.g. in the United Kingdom in [12]. As previously mentioned, BESS are particularly well-suited for frequency regulation due to their rapid response time, high flexibility, and superior energy efficiency [10].

In Europe, ancillary services for frequency control are usually categorized into several reserves [14], including Fast Frequency Reserve (FFR), Frequency Containment Reserves for Normal and Disturbance conditions (FCR-N and FCR-D), and Frequency Restoration Reserve (FRR), both automatic (aFRR) and manual (mFRR). These reserves each help manage frequency anomalies with different time responses and capacities.

Energy systems size and operation optimization models

As energy systems including storage grow exponentially, and numbers of related studies state to optimize the performances. In this context, optimization can have several meanings depending on numerous different factors [15].

The goal of optimization divides models into several categories. Some models focus on financial and economic parameters of the energy system. A very widely recognized subcase here is the cost optimization, which aims to minimize the overall costs, installation and operation. The studies by Nojavan et al. [16], Gupta et al. [17], Han et al. [18], and Rivera-Durán et al. [19] share that common focus on the economic optimization of energy storage systems in microgrids, with the minimization of grid-related costs at the core of their methodologies. Nojavan et al. [16] developed a cost-reliability optimization model that balances energy storage sizing while integrating demand-side management to reduce microgrid operational expenses. Gupta et al. [17] examined the levelized cost of electricity (LCOE) in hybrid renewable-storage systems, highlighting the ability of BESS to mitigate grid dependency and stabilize costs in variable renewable energy environments. Han et al. [18] conducted a techno-economic assessment of PV-BESS deployment, where the investment in storage is optimized to minimize grid reliance and enhance revenue generation under different market participation strategies. Rivera-Durán et al. [19] extended this approach to standalone microgrids, demonstrating how BESS can support fully renewable energy systems by reducing operational costs and ensuring supply reliability in isolated regions. In such optimization problems, core variables are the micro-grid operation cost and the BESS investment cost. An example of trends for this kind of problems is presented in Fig 2.

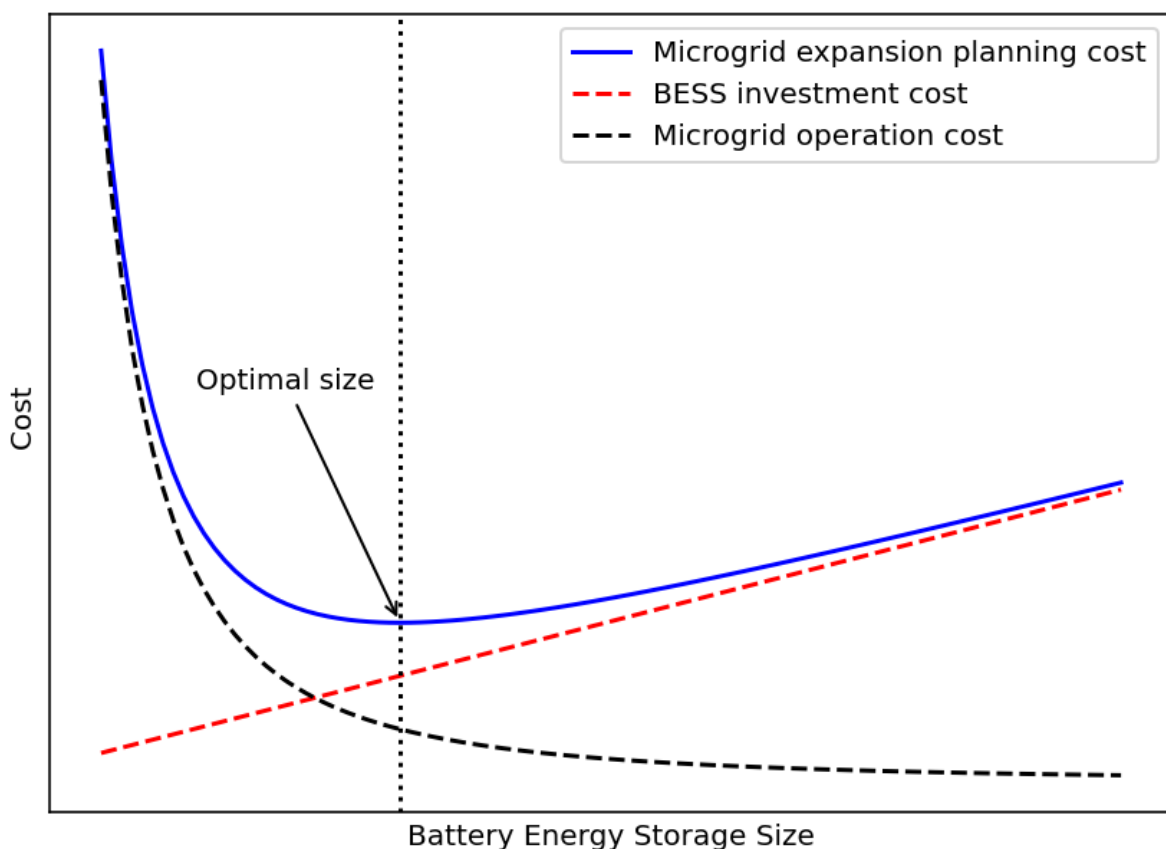


Fig 2: Optimization based on the cost-efficiency of a micro-grid [16]

On the other hand, large-scale systems connected to the grid have at heart to maximize the revenues generated by the addition of an ESS. Zhu et al. [20] studied an ESS with a windfarm that is available to access balancing markets and generate extra revenues.

Non-economic objectives can also be the center of the model or added as secondary objectives in some cases. The focus can be put e.g. on the delivery of the firm and stable power load to the grid as detailed by Gupta et al. [17] and Tejero-Gómez [21], the minimization of carbon dioxide emissions in an energy system with fossil fuel-powered infrastructures as for the Canadian electricity grid studied by Vaillancourt et al. [22] or PV-diesel-BESS systems by Aziz et al. [23] or the maximization of the lifespan of the ESS [16].

Optimization of ESS depends heavily on the object of optimization, the parameter affecting the model. Two main categories of models can be described here: models focusing on the real-time operation of the ESS and models focusing on the sizing of the ESS through its rated capacity or energy stored. The first category usually presents strategies to adapt the operation of the energy system based on the real-time conditions of the connected grid, such as load, frequency, or energy market prices. Zhu et al. [20] describes a strategy to adapt ESS load to the balancing markets prices and power imbalance, whereas Aziz et al. [23] focuses on a dispatch strategy of different energy sources.

ESS sizing models are the other large category. In that case, the optimization is not run in real-time based on parameters varying over time, but time-independent, based on fixed

parameters of the energy system. Blasuttigh et al. [24] and Korjani et al. [25] investigate the sizing at a local scale for self-consumers, whereas Hassan et al. [26] and Liao et al. [27] study it for micro and distribution grids.

While batteries are often discussed in the recent literature, literature shows that similar benefits are studied with other forms of energy storage as well, such as ultracapacitors [28], pumped hydropower storage [29], flywheels, or compressed air energy storage (CAES) for wind and hydropower [30], or thermal energy storage for concentrating solar power (CSP+TES). The longer-duration forms of energy storage also have the potential to offer additional benefits, such as mitigating transmission congestion and enhancing system flexibility [31].

As seen with several forms of energy storage, size optimization strategies are studied under different energy contexts. Some models consider BESS in a standalone configuration connected to a load and/or the grid. In those cases, the BESS is the only energy source except for the grid. Strategies are based on the lowest dependency from the grid for the load and especially on the volatility of the electricity prices. However, models are more and more turning towards hybrid energy systems combining several energy sources at the same location. These approaches are usually constituted of a combination of one or several energy generation systems and an energy storage system. Strategies here consist, when applicable, in tackling the intermittency of a renewable-based power plant to ensure firm power generation, enhancing the auto consumption of a co-located load, and mainly shifting the production of renewable-based power plants to benefit from better electricity prices. The energy sources in hybrid situations are numerous, but mostly renewable. Among the most represented in literature can be found PV studied among others by Blasuttigh et al. [24], Korjani et al. [25] or Hassan et al. [26], wind detailed by Gupta et al. [17], Zhu et al. [20] or Abbey and Joos [28], hydropower [30] but also advanced hybridizations as PV-Wind [32], Wind geothermal [29] or situations with an auxiliary fossil fueled source such as PV-Diesel-BESS [23] and even Wind-PV-Diesel-BESS [33].

Not only do the energy sources differ from one model to another, but so do the electricity transmission and use. The optimal size of BESS varies significantly based on grid configuration, market participation, and operational constraints. Starting from the smallest scale, on an individual level, residential BESS focuses on self-consumption and resilience. Examples of such PV-BESS models are presented and discussed in by Blasuttigh et al. [24] and Korjani et al. [25]. Online tools are also accessible for anyone to assess the optimal BESS size for their situation [34]. On the same local and individual level, large industries use PV-BESS combination to shave their peak demand, ensure a firm production independent from the grid and overall reduce their costs. Some optimization strategies under these circumstances are described by Xu et al. [35] or Wu et al. [36] for large industries, or by Tarray and Martinsen [37] for small behind-the-meter applications.

Microgrids are the next scale broadly studied in the literature. In these contexts, loads from residential, commercial and/or industrial are linked to BESS and energy sources, usually renewable. BESS help to support an island-mode operation and grid independence. Such cases for grids in remote locations are described by Rivera-Durán et al. [19] and Ogunjuyigbe et al. [33].

All these configurations fall under a larger category of BESS implementation, *Behind-the-Meter (BTM)*, in which the BESS is located on consumers' side and tends to enhance self-consumption and energy independence. On the other hand, there are *Front-of-the-Meter (FTM)* BESS, connected to the utility grid side. These kinds of BESS are larger in terms of capacity, big enough to take part in energy markets. Strategies in optimizing those rely on helping integrating renewables, providing frequency regulation services and trading on wholesale markets. Their installation is studied both at the distribution level by Han et al. [18] and Liao et al. [27] and transmission grid by Gupta et al. [17] and Hassan et al. [26].

Lastly, algorithms and methodologies have been developed to achieve size optimization, each with its own strengths and limitations. Some of the most used algorithms across literature are: Dynamic Programming (DP), Linear Programming (LP), Mixed-Integer Linear Programming (MILP) and generally metaheuristic approaches [38]. DP is used mainly for optimal scheduling and operation of BESS, particularly in applications where battery operation and degradation needs to be explicitly modeled over time [20]. Linear Programming is often used for cost-efficiency and revenue maximization in energy trading markets where BESS participates in day-ahead and balancing markets [26]. MILP is widely used for optimal BESS sizing in hybrid renewable energy systems, market participation, and grid support applications where binary or integer decisions (e.g., investment decisions, operational constraints) are necessary [32]. Metaheuristic methods are particularly useful for BESS sizing when the search space is large, nonlinear, or contains multiple local optima. Models including several energy sources, storage and/or large loads usually use this type, such as the PV/Wind/Split-diesel/Battery system studied by Ogunjuyigbe et al. [33] or the university complex studied by Moghimi et al. [39].

BESS operation on energy markets

Overall, the research panel for size optimization of BESS is wide and many models exist. However, due to an even larger number of parameters, configurations and applications, all *cases still don't appear in the literature. An important part included in many models* is the consideration of participation in ancillary services and balancing markets. These markets include energy arbitrage, frequency regulation services (FCR, FCR-D, aFRR, mFRR), reserve markets, and capacity markets. The flexibility of BESS makes it a valuable asset for grid stability, as it can respond quickly to supply-demand fluctuations and provide services such as load balancing, voltage regulation, and black-start capability.

Energy arbitrage involves charging the battery during periods of low electricity prices and discharging when prices peak, aiming to maximize revenue. However, studies such as Zafirakis et al. [13] and Wu et al. [36] demonstrate that the economic viability of arbitrage is highly dependent on market price volatility and battery degradation costs. In many cases, arbitrage alone is not sufficient to justify large-scale BESS investments due to low daily price spreads, as observed in European markets. The profitability of arbitrage also depends on market rules, such as bidding restrictions, settlement periods (hourly vs. 15-minute resolution), and transmission fees, which can significantly impact revenue potential.

One of the challenges identified by Nojavan et al. [16] is the trade-off between increasing BESS capacity for arbitrage and the associated rise in degradation costs. Frequent charge-discharge cycling accelerates capacity fading, leading to higher operational expenses. The research by Serres [40] explores the economic impact of lithium-ion battery degradation in

grid-scale applications, reinforcing the need to optimize battery dispatch strategies to minimize wear while maximizing revenue.

Among all market segments, frequency regulation services (e.g., FCR-D, aFRR, mFRR) have emerged as the most profitable for BESS. Studies such as Villar et al. [14] and Zhu et al. [20] show that FCR-D participation provides stable revenue streams through capacity payments, making it a preferred option for storage operators. Unlike arbitrage, where profits depend on volatile price spreads, ancillary services offer predictable income through pre-contracted capacity bids.

Additionally, BESS is uniquely suited for frequency regulation due to its rapid response time, allowing it to react to grid imbalances within seconds. However, research by Hannan et al. [38] highlights that market saturation in ancillary services may reduce profitability over time, as increased BESS deployment leads to declining clearing prices. The study by Tejero-Gómez and Bayod-Rújula [21] further emphasizes that while BESS is highly effective for frequency control, current market rules do not fully compensate for degradation costs, requiring additional revenue stacking strategies.

Beyond traditional energy markets, BESS is now being explored in new market structures. Alavijeh [41] investigates some of them including:

- Congestion Management: Participating in congestion relief services by redistributing excess generation.
- Local Flexibility Markets: Bidding into localized energy markets to provide demand-side flexibility.
- Capacity Mechanisms: Securing revenue through capacity auctions, ensuring long-term financial stability.

While these opportunities are increasingly being studied, existing literature lacks in-depth techno-economic assessments of how BESS can dynamically allocate resources across multiple market segments. Future studies should develop multi-market optimization frameworks that allow BESS operators to switch between revenue streams in real time, maximizing overall profitability.

Co-location and synergies between PV and BESS

The integration of BESS with PV systems has been widely explored, with research focusing on reducing curtailment, increasing self-consumption, and optimizing power flows between generation and storage. However, while many studies analyze standalone PV-BESS configurations, there is a lack of comparative research on different grid connection strategies.

Many studies focus on behind-the-meter BESS, where storage is used to maximize PV self-consumption and reduce grid reliance. Xu et al. [35] analyze BESS sizing for industrial PV users, showing that battery integration improves energy independence and reduces peak demand charges. Similarly, Blasuttigh et al. [24] explore the economic viability of PV-BESS systems for self-consumption, emphasizing that system profitability depends on battery costs, retail electricity rates, and policy incentives.

While these studies provide valuable insights, they typically assume fixed grid connection conditions and do not explore how different grid integration configurations affect profitability. For instance, research rarely compares dedicated BESS injection to shared grid capacity with PV, the impact of grid congestion on dispatch strategies or the differences between islanded operation and grid-connected flexibility markets.

Few studies focus on grid-connected PV-BESS systems participating in wholesale markets, despite their growing relevance. Tejero-Gómez and Bayod-Rújula [21] analyze PV-BESS operation under monthly fixed output schedules, but do not compare multiple grid access strategies. The work of Gupta et al. [17] discusses the levelized cost of electricity (LCOE) for storage-supported renewables yet does not explore how grid constraints alter optimal dispatch strategies.

A significant research gap exists in analyzing how grid interconnection settings influence BESS dispatch, revenue potential, and market participation opportunities. Future research should consider grid injection limitations and their impact on BESS profitability.

Energy market prices forecasting models for accurate predictions

Accurate price forecasting is critical for optimizing BESS dispatch strategies, particularly for energy arbitrage and multi-market participation. However, most research focuses on short-term price forecasting (minutes to days ahead), lacking detailed long-term hourly price projections.

Common forecasting techniques include:

- Machine Learning (ML) Approaches: Neural networks, support vector machines (SVM), XGBoost (Hannan et al. [38])
- Statistical Models: ARIMA, autoregressive models (Wu et al. [36])
- Hybrid Forecasting: Combining fundamental market models with ML (Gupta et al. [17])

While these methods provide good short-term accuracy, they often fail to capture structural market changes such as policy shifts, renewable penetration growth, and demand evolution. One of the key research gaps is the absence of robust long-term, high-resolution price forecasts. Many studies assume simplified trend-based forecasts, rather than integrating detailed market simulations. Han et al. [18] note that long-term projections are often based on yearly averages rather than granular hourly variations, which can lead to suboptimal BESS dispatch decisions. Future work should focus on developing long-term price forecasting models with hourly resolution.

Weather forecasting models for realistic performances

The generation of weather forecasts is also primordial when running long-term models involving PV plants as their generation and performance will be impacted. Several models can be discussed and found in the literature, from the naive ones to more complex AI-driven models.

One might first think about naive methods such as selecting a specific year and replicating its data for the whole studied period. It is easy to implement but can be problematic because it

introduces the risk of basing system design on abnormal weather conditions. Averaging solar irradiation over the last ten years may also seem like a reasonable approach. However, this method fails to capture realistic weather patterns that affect energy production. In practice, solar generation is not just about the total amount of radiation received over a period, but also about its seasonal, daily, and hourly variations, which impact the BESS operation and potential in this work.

On the other hand, complex and advanced models can be used, such as AI-driven forecasts. Machine learning models can indeed leverage large datasets, including satellite imagery and historical weather patterns, to predict solar irradiation in Europe as studied by Nematchoua et al. [42] or to assess solar power and grid efficiency as described by Bouquet et al. [43]. However, while these models can improve accuracy, they require extensive data processing and may still struggle with long-term variability. Their use adds complexity and longer processing time to the model. Some studies incorporate complete climate change models to project future solar radiation trends. In [44], the projections from the Coupled Model Intercomparison Project, Phase 6 (CMIP6) [45] are used to assess future solar radiation. While valuable for long-term planning and interactions between weather parameters, these models are heavy in terms of data processing and calculations to predict all characteristics of local and global climate.

The Typical Meteorological Year (TMY) model is a compromise between using raw historical data and building a representative and realistic model. A TMY is a synthesized dataset representing typical climatic conditions for a specific location over a one-year period. It comprises hourly values of different meteorological parameters, such as solar radiation and temperature. These datasets are constructed by analyzing long-term historical weather data, over at least a decade. The process consists in selecting individual months from different years that best represent median or average conditions for each respective month. For instance, January might be selected from 2019, February from 2021, and so on, to form a composite year that reflects typical weather patterns without the anomalies of any single year.

The methodology for creating TMY datasets is detailed in international standards, such as ISO 15927-4, which outlines the procedures for selecting and assembling data to ensure it accurately reflects typical meteorological conditions for a given location. This involves statistical analysis to identify months that closely match long-term averages and other criteria, ensuring the composite year is as representative as possible. [46]

Battery degradation models

Battery degradation is also a key point in models, as it has an important impact on performance, especially on the long-term. Therefore, degradation is crucial to implement in *the sizing process*. *Few studies still don't consider it and even though several studies have introduced battery degradation in their models, linear degradation assumptions are usually applied.* [37] More complex and realistic degradation would be necessary to ensure more precise results, especially in the context of trading on energy markets, such as described by Serres [40] and Munukutla [47]. A multi-stage degradation model will be used in this work based on [47].

Research gaps

Overall, despite the number of studies on the optimization of BESS sizing and operation, several significant gaps remain. First, few studies thoroughly address the impact of different grid connection strategies on the profitability of PV-BESS systems, particularly when comparing dedicated injection versus shared capacity models. Moreover, most economic models rely on short-term market price forecasts without incorporating realistic long-term hourly predictions, which are crucial for accurate planning. Battery degradation effects, although acknowledged, are not systematically integrated into multi-market optimization strategies. Finally, the lack of reliable long-term weather modeling (capturing seasonal and climate variability) introduces bias in the assessment of PV-BESS performance. This thesis aims to include these gaps.

3. Scope and Research questions

Research questions

The objective of this study is to develop a BESS sizing tool for different co-location configurations with a large-scale PV power plant. This study focuses on finding the optimal battery capacity allowing the maximum profitability when operating on different energy markets.

The following questions will be covered through this work:

- How can the optimal size of a Battery Energy Storage System (BESS) be determined for co-location with a photovoltaic (PV) power plant to maximize operational efficiency and profitability?
- How can a co-located BESS contribute to grid stability while maximizing its financial returns in energy and ancillary service markets?

Scope

This study will focus on the development of the sizing tool. The studied technology is the Li-ion - LFP battery as this is the main one on large-scale markets.

The goal of the optimization in this thesis is the size of the BESS, and not its real-time operation. Therefore, the operation will follow simple assumptions based on the maximization of revenues. *Further real-time operation modes won't be covered by this work.*

The optimization implemented in this work is a dual-loop optimization. It involves an outer loop running a discrete parametric optimization on battery capacity to maximize profitability over the lifetime, and an inner loop running on a linear programming optimization model for the daily operation of the battery.

The daily optimization process will be coupled with a multi-stage degradation model by Munukutla [47], which runs several optimization loops in order to minimize the impact of degradation on revenues and increase the lifespan of the battery.

The revenues will be coming from 2 different energy markets, through different products according to countries:

- Day-ahead arbitrage
- Frequency Containment Reserve - Disturbance (FCR-D) Up
- Frequency Containment Reserve - Disturbance (FCR-D) Down
- Symmetrical FCR-D Up/Down

Overall, this work's novelties are:

- The provision of a complete tool, including the building of simple forecasts for both electricity markets prices and PV generation in order to simulate long-term operation,
- An assessment of different PV-BESS co-location types from a grid connection perspective,
- The implementation of 15min resolution for energy markets price, while still allowing for calculation on an hourly basis.

4. Methodology

This chapter will present the methodology followed in this study and the tool developed. First, an overview of the tool presenting its features, mechanisms, inputs and outputs is described. The second section focuses on the building of forecasts for the PV generation and the electricity prices both on spot and FCR-D markets. A third section dives into the multi-stage optimization process run to size the battery. Finally, a fourth section presents the case study chosen for the application of the tool in this study.

4.1. Overview of the tool

The goal of the tool developed in this work is to compute the optimal size of a BESS when co-located with a PV power plant. The optimum size is the capacity allowing for the maximum profitability over the life of the battery.

The main features of the tool are:

- PV generation forecasting specific to the location and characteristics of the PV plant
- Simple electricity markets prices forecasting
- Daily operation optimization on energy markets
- Multi-stage battery degradation model
- Several co-location scenarios for PV and BESS

The tool follows the following process when running:

- Build PV generation forecasts
- Build simple electricity markets prices forecasts
- Compute pre-calculations based on the input data
- Optimize daily operation based on market entry for a fixed battery capacity
- Iterate for the whole range of capacities
- Economically assess the operation
- Evaluate the optimal battery size

An overview of this process is illustrated in Fig 3.

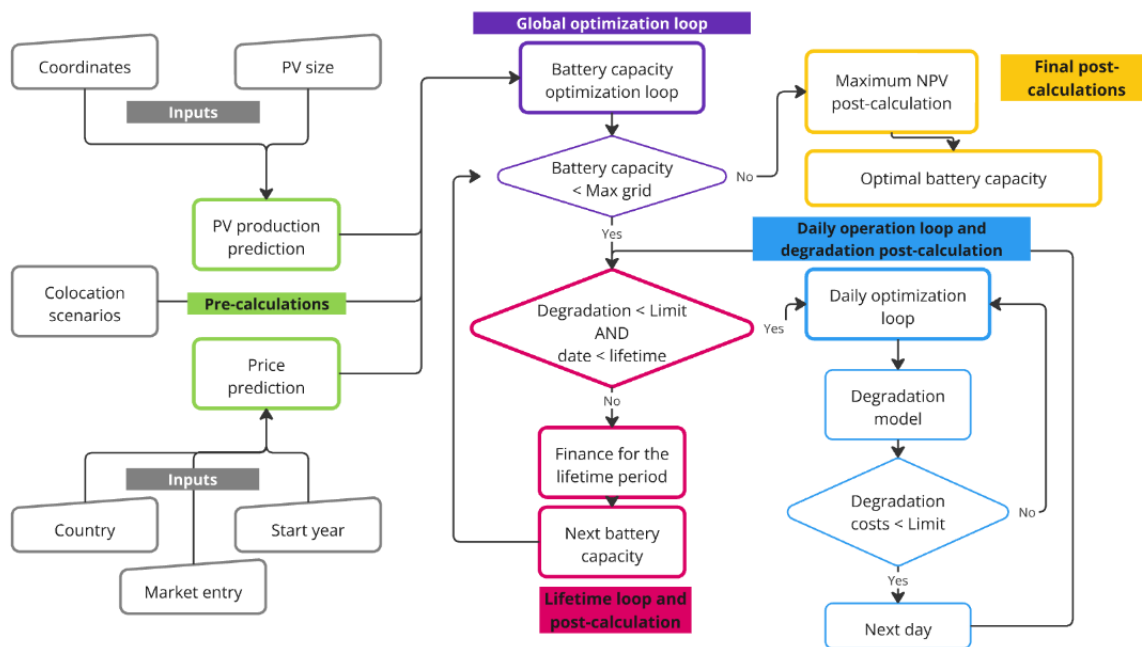


Fig 3: Methodology of the tool

The tool requires a number of inputs that are necessary for it to run, divided into several different categories:

- Location-specific,
- Grid-related,
- Financial related to the project economy,
- PV-related,
- Market prices-related,
- Scenario and optimization-related

First are site-specific inputs, such as the location, which is mandatory and includes both the country and precise geographical coordinates. This ensures that all calculations and forecasts are location-specific, considering regional factors such as solar irradiance and grid conditions.

Another crucial input category is grid-related data, which is also mandatory. This includes the available capacity at the connection point, defining the grid constraints for the system, as well as the grid connection costs covering both capital expenditure (CAPEX) and operational expenditure (OPEX). These costs are essential for evaluating the financial viability of the project. Similarly, battery data must be provided, including the CAPEX and OPEX associated with the energy storage system, as this significantly impacts the project's overall cost and profitability.

For the PV system, certain inputs are mandatory while others are optional. Users may input personalized module specifications and PV generation data if available, although these are optional. However, defining the AC/DC ratio and the nominal AC power of the system is mandatory, as they are essential for system sizing and performance calculations. Additionally, pricing-related inputs allow for more detailed financial projections. Users can include price forecasts for both spot and FCR-D electricity markets, with the appropriate resolution and price

trends per year, both of which are optional but highly useful for financial modeling and revenue estimation.

The tool also provides optimization settings that influence system operation and performance. Users can specify the maximum number of battery cycles per day, an optional parameter that affects battery degradation and operational strategy. Additionally, the tool supports scenario selection, allowing users to explore different optimization scenarios based on the wanted depth of interconnection between the PV plant and the BESS.

The outputs of the tool provide actionable insights for decision-making. One of the primary results is the optimal battery energy storage system (BESS) size, ensuring the best balance between cost and performance. Additionally, the tool calculates key financial metrics, including net present value (NPV), yearly cash flow, and internal rate of return (IRR), offering a clear picture of the project's economic viability. For further financial analysis, a detailed NPV assessment across all tested battery sizes is provided and a detailed distribution of incomes per year in the optimal configuration.

The inputs and outputs are summarized in Table 1:

Table 1: Inputs and outputs of the tool

Category		Variables	Units	Type
Inputs	Location	Country	-	Mandatory
		Coordinates (Latitude, Longitude)	Decimal degrees (WGS84)	Mandatory
	Grid related data	Capacities on the grid (consumption and injection)	MW	Mandatory
		Grid costs (CAPEX / OPEX)	€/MW	Mandatory
	Battery data	CAPEX / OPEX	€/MWh	Mandatory
		Lifetime	Years	Mandatory
	Financial data	Weighted Average Cost of Capital (WACC)	%	Mandatory
		Depreciation time	Years	Mandatory
		Inflation	%/year	Mandatory
		Tax	%	Mandatory
	PV data	Nominal AC Power	MWp	Mandatory

		AC / DC ratio	-	Mandatory
		Personalized PV module data	See 4.2.2.1	Optional
		Personalized PV generation forecasts	MW AC	Optional
	Market data	Market	Spot market or FCR-D	Mandatory
		Price trends per year	SM: €/MWh FCR-D: €/MWh/h	Optional
		Price prediction with resolution	SM: €/MWh FCR-D: €/MWh/h	Optional
	Optimization	Maximum cycles per day	-	Optional
		Maximum degradation	-	Optional
		Starting year	-	Mandatory
		Scenario	1, 2 or 3	Mandatory
Outputs	Technical	Optimal BESS size	MW	
		Degradation over lifetime	-	
	Financial	Associated NPV	k€	
		Associated IRR	%	
		Associated yearly cashflow	k€ / year	
		NPV per battery capacity	k€	

4.2. Inputs and pre-calculations

This section focuses on the description of the methodologies followed to create the different forecasts necessary for the tool: first the PV generation forecasts and then the energy market price projections. A third part describes the co-location configurations investigated in the tool and the characteristics they have for the BESS and its grid connection.

4.2.1. PV forecasts

This section describes the methodology followed in this work to create high-resolution PV generation forecasts that can be used in the tool for the daily operation of the BESS.

The tool described in this study is designed to build PV generation forecasts based on the following methodology:

- Extraction of a Typical Meteorological Year (TMY) weather profile
- Creation of weather forecasts for 2050 based on TMY data
- Application of the PV module generation model
- Application of the PV inverter performance model

This methodology is detailed in Fig 4:

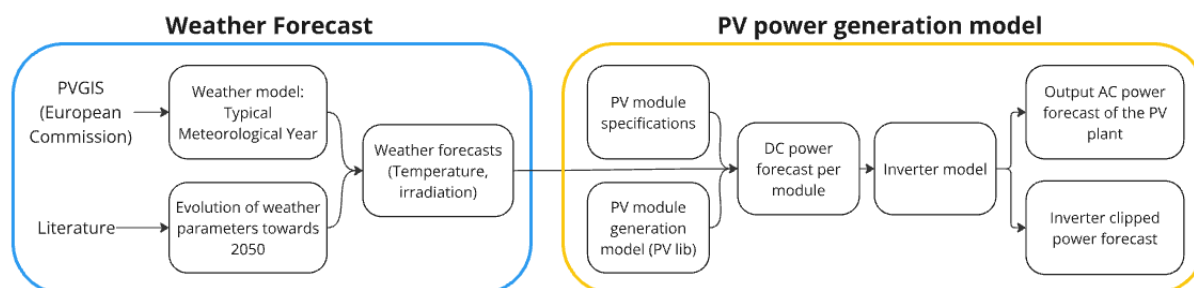


Fig 4: PV generation forecasts methodology

4.2.1.1. Weather forecast

As explained in the literature review, the model used as a basis for weather profile is the Typical Meteorological Year (TMY) model. Following the methodology described by Huld et al. [46] and Wilcox and Marion [48], the calculation of the TMY has been implemented in PVGIS, Photovoltaic Geographical Information System, a tool developed by the European commission providing information on solar radiation and photovoltaic system performance. [49]

Given the specific location of the co-location project, i.e. latitude and longitude, PVGIS extracts the corresponding weather data. The data is given as an hourly profile for one year.

The TMY data is composed of three sub-datasets:

- The Global Horizontal Irradiance (GHI) on a horizontal plane at the location per hour in W/m²
- The Direct Normal Irradiance (DNI) reaching the panels per hour in W/m²
- The average ambient temperature per hour in °C

After having modeled a typical year, the data is adapted to consider the evolution of climate *over multiple years' time scale*.

The TMY obtained previously serves as a basis and is scaled up according to irradiation and temperature evolution in the future. The timescale considered will be until 2050 as the lifetime of a BESS is about 15 years, allowing for flexibility in the starting year.

Long-term evolution of irradiation quantities, such as Global Horizontal Irradiance and Direct Normal Irradiance, are presented by Huber et al. [50]. In Northern and Central Europe, GHI and DNI are respectively said to increase by 3% and 12% by 2039 compared to 1990 levels.

Long-term evolutions of temperature are established in [42] with the help of several deep-learning algorithms. Evolutions towards 2050 are presented based on different IPCC scenarios for climate trajectories. Considering the intermediate scenario provided by the IPCC, Central and Northern Europe will face small variations in temperature, increasing from 12.6 °C in 1990 to 14.26 °C by 2050.

To apply the evolutions on GHI and DNI from [50] and temperature from [42] to the TMY profile, the increase rate will be considered the same every year. Therefore, increases of respectively 0.207%, 0.064% and 0.243% per year until 2050 for temperature, GHI and DNI will be applied. Values and increase rates are presented in Table 2.

Table 2: Evolution of irradiation and temperature towards 2039 and 2050 [42] [50]

Parameters	Temperature (°C)		GHI (W/m ²)		DNI (W/m ²)	
	1990	2050	1995	2039	1995	2039
Year						

Values	12.6	14.26	274.22	282.20	177.78	198.31
Increase per year i_X	0.207%		0.064%		0.243%	

The data for the coming years are obtained by applying these increases to the TMY profile following Eq 1 for parameter X, i.e. either Temperature, GHI or DNI:

$$X_n = X_0 \cdot (1 + i_X)^{n-n_{ref}}$$

Eq 1

Where:

- n is the current year
- n_{ref} is the reference year, i.e. 2024
- X_n is the parameter value for the given year
- X_0 is the parameter value for the reference year, i.e. from the TMY profile
- i_X is the annual increase rate for parameter X

4.2.1.2. PV power generation model

This part focuses on the generation of a PV generation profile based on the weather forecast given by 4.2.1.1. Weather forecast or provided by the user.

Module specifications input

In order to compute correctly and precisely the performance of the PV plant, the technical specifications from the installed module are necessary. The module can be a user input and therefore, specifications must be provided.

If not provided, the specifications from one of the most common modules on the European market will be used, CS1U-400MS by CanadianSolar [51], which represents nearly 20% of the installed modules in large-scale PV power plants on the European market in 2024 [52].

The important parameters from the specifications are:

- The nominal maximum power P_{max}
- The optimal operating voltage V_{mpp}
- The optimal operating current I_{mpp}
- The open-circuit voltage V_{oc}
- The short circuit current I_{sc}
- The temperature coefficients $\alpha_{I_{sc}}, \beta_{V_{oc}}, \gamma_{P_{max}}$ for I_{sc} , V_{oc} and P_{max}

The data provided for the PV module are given in Table 3:

Table 3: Standard PV module specifications [51]

Under Standard Test Conditions ($G_{ref} = 1000 \text{ W} \cdot \text{m}^{-2}$, $AM_{ref} = 1.5$, $T_{cell,ref} = 25^\circ\text{C}$)		
Nominal maximum power P_{max}	400	W

Optimal operating voltage V_{mpp}	44,1	V
Optimal operating current I_{mpp}	9.08	A
Open-circuit voltage V_{oc}	53.4	V
Short circuit current I_{sc}	9.60	A
Temperature coefficients		
$\alpha_{I_{sc}}$	+0.05	% / °C
$\beta_{V_{oc}}$	- 0.29	% / °C

PV module generation model

The models applied in this study to estimate the generation of a PV module, and the operation of an inverter are based on existing models from literature [53]. These models are implemented in a Python library called PVlib [54], used for the power generation modelling in the tool.

A general overview of the mathematical-physical model is presented in this section.

The power delivered by a PV module can be modeled with an equivalent circuit as presented in Fig 5. [55]

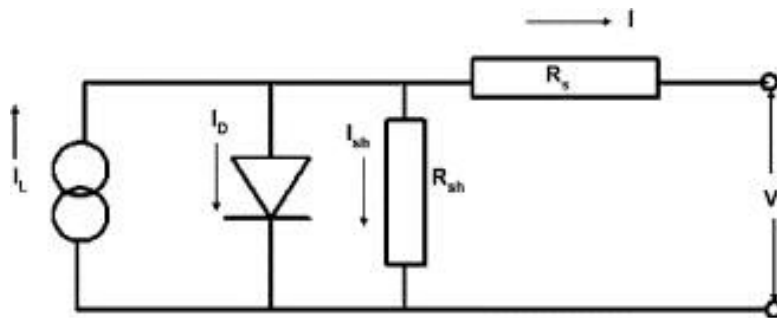


Fig 5: PV module electrical equivalent circuit [55]

At fixed conditions of cell temperature and solar irradiation, the relationship between current and voltage is expressed in Eq 2:

$$I = I_L - I_0 \cdot \left[e^{\frac{V+IR_s}{a}} - 1 \right] - \frac{V+IR_s}{R_{sh}}$$

Eq 2

Where:

- I_L is the light current in A,
- I_0 the diode reverse saturation current in A,
- R_s the series resistance in Ω ,
- R_{sh} the shunt resistance in Ω ,
- a the modified ideality factor in V^{-1} .

These five unknown parameters are evaluated by replacing the values of current and voltage from the specifications in their respective configurations (open circuit, short circuit, maximum and power point). This gives the I-V curve for the module under standard conditions.

The irradiation and temperature impact the current and voltage and therefore the output power. All 5 parameters from the equation evolve with temperature and irradiation, modelling their variation allows for the calculation of the performance of the module under precise conditions. The methodology described by De Soto et al. [53] and implemented in the Python library *PVlib* accounts for those advanced variations. Hence, the detailed process won't be described in this part.

From the current-voltage curve at operating conditions, the maximum power point is extracted, i.e. the (I, V) couple such that the output power is maximum:

$$P_{mpp,mod} = I_{mpp} \cdot V_{mpp} = \max(I \cdot V) \quad \text{Eq 3}$$

Solar field expansion

The total DC output power of the whole solar field is given by the number of PV modules on the plant in Eq 4:

$$P_{DC} = N_{modules} \cdot P_{mpp,mod} \quad \text{Eq 4}$$

Inverter model and output

The Inverter model is based on the model provided by Driesse in [56] and used in Python library *PVlib*. [54] It is based on the analysis of the inverter performance database from the California Energy Commission. The AC output P_{AC} is given as a function of the DC input power P_{DC} in Eq 5:

$$P_{AC} = \begin{cases} \eta P_{DC} & \text{if } 0 < P_{DC} < P_{DC,0} \\ P_{AC,0} & \text{if } P_{DC} \geq P_{DC,0} \\ 0 & \text{if } P_{DC} = 0 \end{cases} \quad \text{Eq 5}$$

Where:

- $P_{AC,0}$ is the maximum AC output of the inverter,
- $P_{DC,0}$ is the associated maximum DC input that can be handled,
given by $P_{DC,0} = \frac{P_{AC,0}}{\eta_{nom}}$ with η_{nom} the nominal inverter efficiency
- η is the efficiency of the inverter for the given P_{DC} input

The efficiency η is given by Eq 6:

$$\eta = \frac{\eta_{nom}}{0.9637} \left(-0.0162 \cdot \zeta - \frac{0.0059}{\zeta} + 0.9858 \right) \quad \text{Eq 6}$$

$$\text{where } \zeta = \frac{P_{DC}}{P_{DC,0}}$$

In parallel, the DC power clipped by the inverter when the input exceeds the limit $P_{DC,clip}$ is given by Eq 7:

$$P_{DC,clip} = \min(0 ; P_{DC,0} - P_{DC})$$

Eq 7

4.2.1.3. Custom input forecasts

As seen on Fig 4, the forecasts are built in two steps: first a weather forecast and then the final PV generation forecast. If the user has their own forecasts for one of these two, the sizing tool developed in this thesis can integrate them as data input. Preprocessed forecast data can be incorporated into the model at different levels and under some conditions:

1. Weather Forecast-Based Input:

The weather forecasting part is preprocessed by the user and the weather forecast directly injected into the PV generation part. In this case, the weather dataset must include two key meteorological parameters:

- Global Horizontal Irradiance reaching the PV panels in W/m²
- Direct Normal Irradiance in W/m²
- Ambient temperature in °C

Both parameters must be provided as hourly forecasts spanning the entire 15-year operational lifetime of the BESS. These inputs are essential for accurately modeling PV module performances.

2. Direct PV Power Production Forecasts:

Alternatively, users can supply direct projections of the PV plant's hourly energy production over the BESS lifetime. In that case, the methodology described in this section won't be applied and the forecasts used directly for the daily operation of the BESS. This PV dataset must include:

- Gross DC power output from the PV field in W
- Net AC power output after inverter conversion in W

The AC production forecast is used to determine the grid capacity utilization by the PV plant, while the DC production forecast is used to estimate the amount of curtailed solar power due to inverter limitations. As with the weather-based approach, these forecasts must be hourly and cover the full 15-year BESS lifetime to ensure accurate system performance modeling.

4.2.2. Price forecasts

Price predictions are a critical input of the sizing model, as they are the direct image of the project revenues.

As for PV production forecasts, the tool requires input a dataset of prices for the whole lifetime of the battery. The regular time resolution for market prices is 1h. Depending on the country, a time resolution of 15 minutes can be used. Besides, more and more countries are turning towards a shorter time resolution of 15 minutes. Therefore, the choice of the time resolution

will be an input parameter, to allow its use on every market and be adaptable to evolving market features.

The tool requires prices for two different electricity markets, based on the two main activities of the BESS, arbitrage on the spot market and ancillary services.

This section will first describe these two operations for the BESS, arbitrage and FCR-D participation, and then present the methodology followed to create long-term prices forecasts for those two electricity markets.

4.2.2.1. Wholesale market / Spot market

The spot market is the main electricity market where electricity is bought and sold prior to delivery time. It is divided into different markets depending on the time before delivery:

- Day-Ahead (DA): Participants submit offers to trade electricity for each time period (1h or 15min depending on the country) of the next day. The closing prices are determined by the prices of the last offer needed to reach demand-supply equilibrium.
- Intra-Day (ID): Open from the closing of DA and until a few minutes before delivery time, participants can adjust their positions based on forecast errors or sudden changes.

A common trading strategy for BESS is arbitrage and consists in taking advantage of the battery flexibility to buy electricity to charge it when prices are low and sell it back by discharging it when prices rise.

As input in this thesis's model, the wholesale market price is considered the clearing price at the end of the Day-ahead auction.

4.2.2.2. Frequency Containment Reserve - Disturbance (FCR-D)

Frequency regulation is a key issue for transmission and distribution system operators (TSO-DSOs). In most European countries, the frequency of the grid is maintained at 50Hz, with minor fluctuations. This state is kept as long as power demand meets power supply. However, events can put the system in imbalance. Overproduction will make the frequency rise over 50Hz, whereas overconsumption will make it drop below. To overcome such events and their potentially large consequences, imbalance markets have been created. Their purpose is to ensure that capacity is reserved on the grid to tackle frequency rises or drops as soon as they occur.

Several markets exist with different focuses:

- Frequency Containment Reserves (FCR), with very short time response, for real-time adjustments,
- Frequency Restoration Reserves (FRR), longer activation time, when imbalance persists after FCR activations,
- Replacement Reserves (RR), for longer and larger imbalances.

The main imbalance market accessed by BESS is the FCR as they can be arbitrated very fast, within seconds. Due to the limited size of grid-scale BESS built today, their participation in

FRR or RR is still sporadic, these markets being covered mostly by large thermal or hydro plants, or large industrial sites.

The FCR market is divided into 2 subcategories, FCR-N and FCR-D, respectively for Normal and Disturbance. FCR-N tackles real-time fluctuations within a range of 0.1 Hz from the nominal frequency of 50Hz. FCR-D is activated once this threshold is reached, aiming to bring the frequency back to normal or at least contain the imbalance until the secondary reserves (FRR) are operational.

This thesis will consider the participation of the BESS in this second market, FCR-D.

Two subproducts are available on the FCR-D market:

- Up, whose purpose is to increase the frequency when it falls under 49.9Hz, by reducing consumption or adding new generation capacity,
- Down, whose purpose is to reduce the frequency when it climbs over 50.1Hz, by increasing consumption or reducing generation.

In Europe, Nordic countries (Norway, Sweden, Finland, Denmark) allow asymmetrical bidding on these two products, i.e. different capacities bid on each one, while continental Europe requires symmetrical bidding, i.e. same capacity bid in both directions.

The way the FCR-D market works is through bids. Prior to the auction, the TSO fixes a value of the estimated need for reserve capacity for the time period. Once the auction is open, energy actors set bids with a capacity and a price. After closing, the TSO selects bids starting from the lowest bid price and until fulfilling the initial need. The last selected bid fixes the *remuneration price for all selected bids. This process is called "pay-as-cleared". Therefore, all selected actors get the same remuneration regardless of their initial bid.*

An important feature is that the remuneration accounts only for the capacity reserve, in €/MW/h, and that in case of activation the delivered or consumed energy won't be remunerated.

The activation of the reserve follows a proportional pattern within its activation range: starting from a variation of $\pm 0.1\text{Hz}$ with a 0% activation, up to $\pm 0.5\text{Hz}$ and a full 100% activation. The activated power as a function of the frequency change is given in Fig 6.

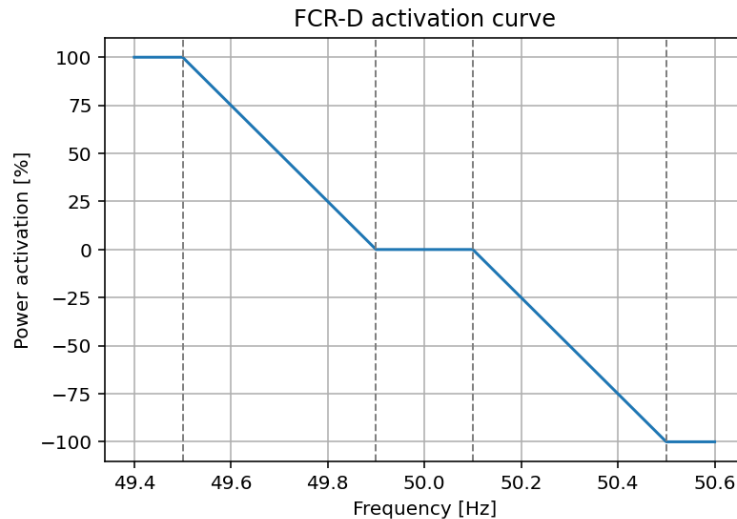


Fig 6: FCR-D activation as a function of the frequency

Participation in this market, however, follows a set of common regulations in most European countries. The minimum bid on FCR-D is 1 MW, meaning that smaller actors must associate with an aggregator to take part.

As an input in the tool, FCR-D prices will be considered the clearing price.

4.2.2.3. Simple Forecasting Model

The following part will focus on a methodology to build price forecasts for the spot market and FCR-D market, with the specified time resolution as input, as seen in the flowchart in Fig 7.

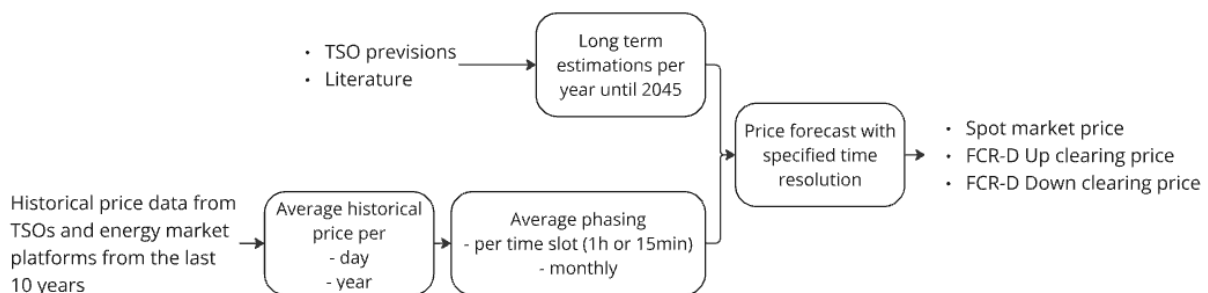


Fig 7: Flowchart of the price forecasting model

Building precise forecasts for such short time resolution is a complex task, therefore, forecasts are usually long-term trends, predicting an average evolution towards a later target value.

To recreate more precise profiles, variations are applied.

Kiesel [57] suggests a method to construct hourly profiles based on seasonality and variations at different scales.

The model includes variations on two main levels:

- Seasonality over the year: Natural phenomena such as temperature variations between seasons induce changes in demand and generation, impacting prices. Social parameters such as holidays periods can also impact the prices.
- Seasonality over a day: Daily economic activities shape the curve of demand over a day. Two peaks are usually observed, one around 8 in the morning and a second

around 18, respectively at the beginning and end of a typical workday. Prices tend to be lower in-between, especially at night.

Historical data reflect these global seasonal trends, so they will be the first source to build phasing models.

Phasing is the mathematical parameter used to illustrate variations. It is defined for a specific time within a variation period, as the ratio of the price for the specific time over the average price for the variation period, as follows in Eq 8.

$$phasing(t) = \frac{price(t)}{price_{av,period}}$$

Eq 8

Two situations will occur: phasing over the day with a time resolution Δt and monthly over the year.

Final phasing are generated by calculating the average phasing over the last 10 years, for both situations. The figures Fig 8(a) and (b) show examples of respectively monthly and hourly phasing.

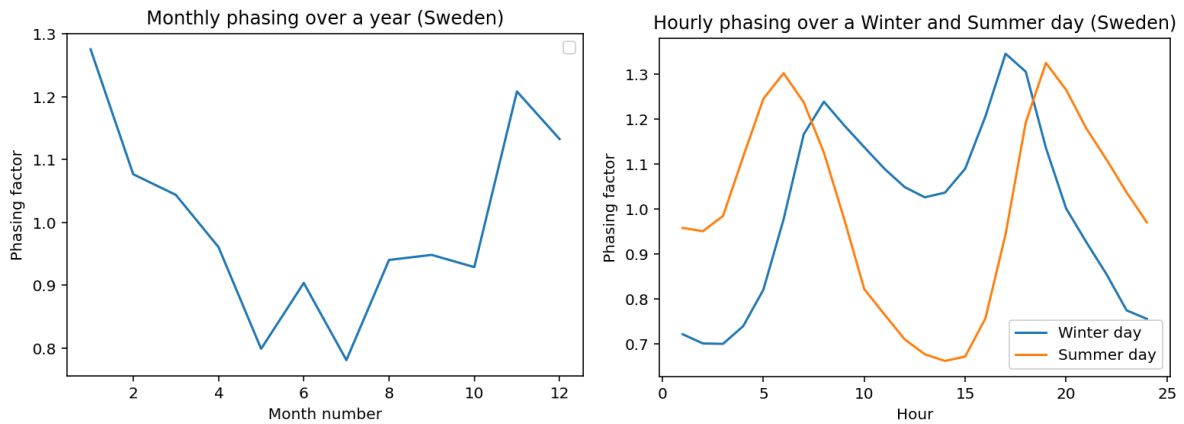


Fig 8 (a)(b): Price phasing over a year (a) and a day (b) for Sweden

Final price forecasts are generated with the phasing and the forecasted average hourly price per year. The price for a given year Y , month M , season S and hour H is given by Eq 9:

$$price(Y, M, S, H) = price_{average}(Y) \cdot phasing(M) \cdot phasing(S, H)$$

Eq 9

4.2.3. Scenarios

Three scenarios are implemented and studied in the sizing tool. These scenarios cover different levels of co-location and hybridization between the PV plant and the BESS. The three scenarios are described as follows:

Scenario 1: Standalone BESS connected to the same grid connection point as the PV

Scenario 2: Co-located BESS sharing a single grid connection with the PV

Scenario 3 : Hybridized BESS with shared connection with PV and interactions

All scenarios share common characteristics and assumptions.

- The PV plant and the BESS are connected on an AC bus. Each asset is running on a separate DC level and has its own DC/AC inverter connected to the bus and to the grid. In this configuration, both assets can inject and consume on the grid. The grid configuration is illustrated by Fig 9.

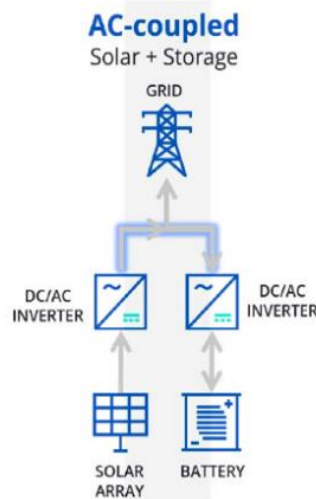


Fig 9: AC-coupled grid connection of PV plant and BESS

- The PV plant and the BESS are, under all three scenarios, kept as two separate assets, owned by two separate entities or SPVs.
- The grid connection is divided into 2 grid allowances, one for injection and one for consumption. On the consumption side, as the PV plant does not consume any electricity, no limitations are applied, and the BESS can use all the capacity it has been assigned. Therefore, the available capacity in consumption is always the grid capacity $C_{grid,cons}$ in all scenarios.
- The injection part is dependent on the PV generation and the configuration and is described for each scenario.

Scenarios are detailed further below.

Scenario 1

This scenario is considered the base case and will be used as a comparison reference for the advanced ones. In this situation, the co-location is purely geographical, both assets are standing next to each other. The connections to the grid are done at the same point, same substation, but the PV and the BESS both have their own assigned capacity on it. No interaction between them is considered.

This configuration can be referred to as “added BESS capacity”. The PV plant is indeed already connected to the grid and has been assigned a maximum capacity to inject, $C_{PV,inj}$, equivalent to its nominal power $P_{PV,nom}$. The BESS would here come on top of the PV with a new grid capacity assigned, as would any other asset connecting to the grid.

The BESS is therefore assigned a fixed capacity to deliver services to the grid, independent of the time of the day. This fixed capacity allowance is defined as the difference between the

total grid capacity on the connection point $C_{Grid, inj}$ and the nominal power of the PV plant $P_{PV, nom}$ given in Eq 10:

$$C_{available, inj, s1}(t) = C_{Grid, inj} - P_{PV, nom} \quad Eq 10$$

The Fig 10 below shows the distinction between the two injection range allowances for the PV plant and the BESS.

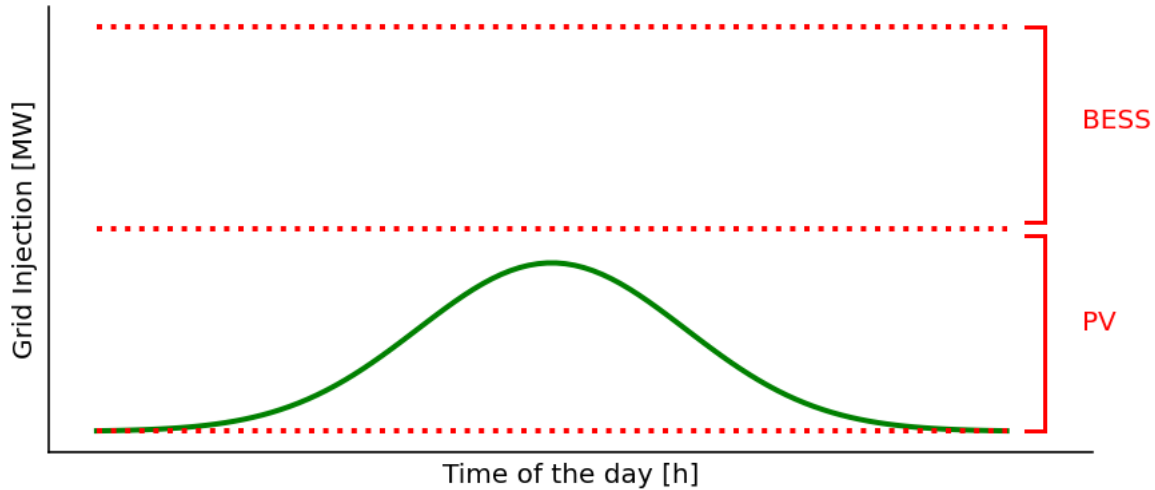


Fig 10: Grid connection capacity repartition between PV and BESS in scenario 1

In this scenario, the PV plant has a fixed assigned grid capacity for injection, equivalent to its nominal power $P_{PV, nom}$. The BESS is assigned the difference with the maximum for injection on the grid $C_{Grid, inj}$. This assigned capacity on the grid is fixed and will remain the same for the whole operating period of the BESS. Its value in that case is time independent and the same for every timeslot t , given in Eq 11:

$$C_{available, inj, s1}(t) = C_{Grid, inj} - P_{PV, nom} \quad Eq 11$$

However, this assigned grid allowance may not be fully used by the BESS, depending on its own technical capacity. If the grid capacity is higher than the technical capacity of the BESS, the battery will simply operate within its own whole range. On the other hand, if the BESS capacity is higher than what is available on the grid, it will operate in the available range. Overall, the smaller quantity among these two will be the limiting factor and set the maximum usable capacity for the BESS, as seen in Eq 12:

$$C_{usable, x}(t) = \min(C_{BESS}; C_{available, x}(t)) \quad \text{and } X \in \{inj, cons\} \quad Eq 12$$

The Fig 11(a) and (b) show the two possible cases in scenario 1 in a given situation of a 6MW total capacity on the grid connection point, 4 MW of which are dedicated to the PV plant. Cases (a) and (b) illustrate situations with a BESS of respectively 1.5MW and 2.5MW capacity.

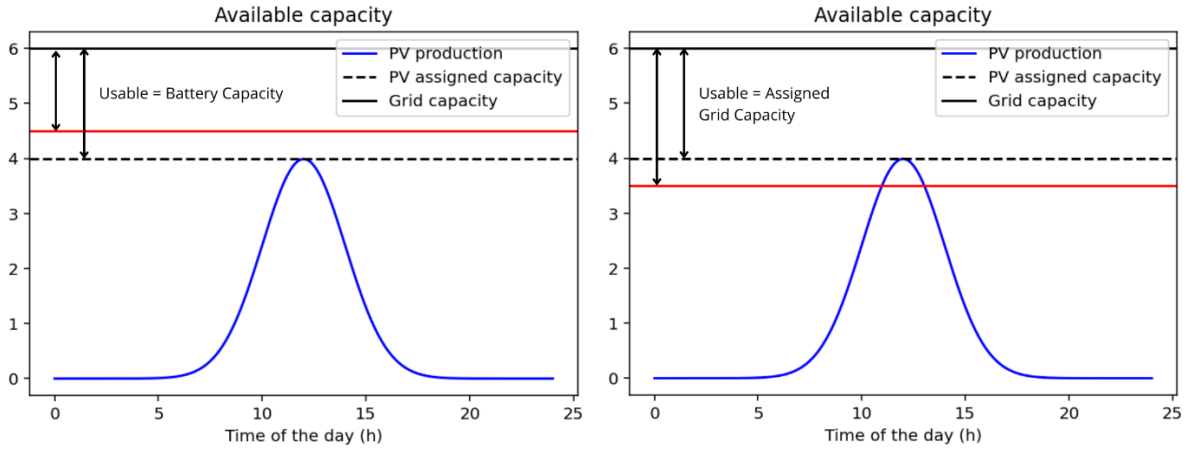


Fig 11(a)(b): usable BESS capacity under scenario 1 for a 1.5MW BESS (a) and 2.5MW BESS (b)

Scenario 2

In this scenario, the co-location is dual. The PV plant and the BESS are again geographically at the same place, but they are also sharing a common grid connection capacity. This configuration can be referred to as “shared PV-BESS capacity”.

The BESS still only operates on grid services and energy markets and therefore charges and discharges solely on the grid, not from the PV. This configuration implies that the PV can only deliver its production to the grid by selling it. This makes the relationship between the PV plant and the BESS a “master-slave” relationship, with the PV being the master. This means that the PV has the priority to inject on the grid while the BESS can deal with whatever is left from the common grid allowance at that specific time.

Under this configuration, the BESS does not have a fixed grid capacity reserved, but a variable one based on the time and the PV production. This allows the BESS to access a larger range of opportunities. As the PV plant injects only throughout daytime, the BESS can have access to the whole reserved grid capacity the rest of the time to take part in ancillary services or arbitrage. Overall, the BESS gets access to a larger capacity range than in scenario 1 anytime the PV plant does not deliver its nominal power, which is most of the time.

The actual availability in injection is defined as the difference between the grid capacity and the PV generation for every timeslot, as seen in Eq 13 **Erreur ! Source du renvoi introuvable.**:

$$C_{available, inj, S2/3}(t) = C_{Grid, inj} - P_{PV}(t)$$

Eq 13

The new grid capacity repartition is shown on Fig 12 below.

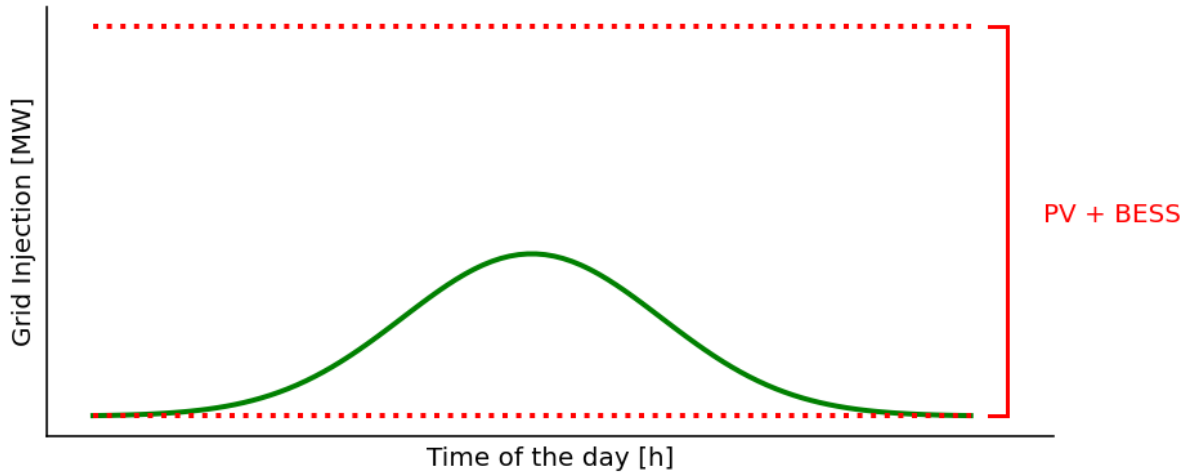


Fig 12: Grid connection capacity repartition between PV and BESS in scenario 2

As mentioned in Scenario 1 and described in Eq 12, the BESS might be technically limited in this available capacity on the grid. The Fig 13 displays the variation in usable capacity over a day in scenarios 2 of shared grid connection. The situation is again a 6MW grid connection shared between PV and BESS, a PV plant with a nominal power of 4MW and a battery capacity of 3MW. During hour $t=2$, at night, the usable capacity is limited by the BESS size, whereas at noon, the limitation comes from the availability of the grid.

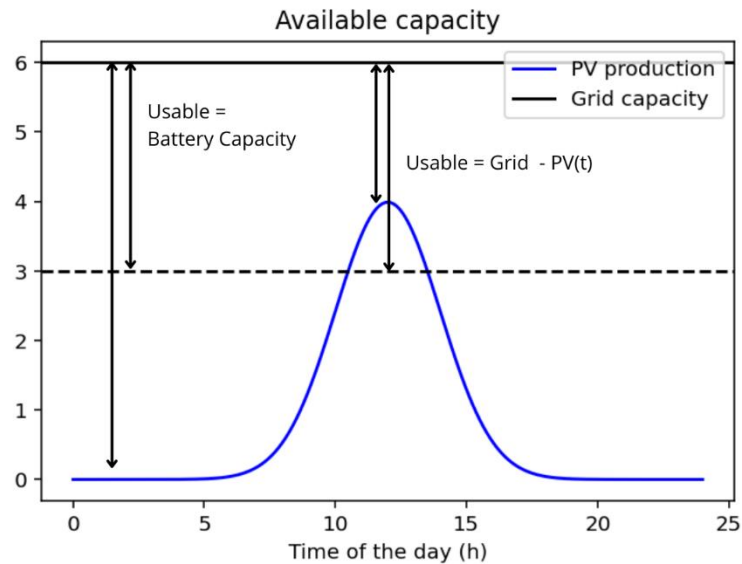


Fig 13: Usable capacity for the BESS over time in scenario 2

Scenario 3

This last scenario investigates a hybridization between the PV plant and the BESS. The co-location level is the same as in scenario 2, i.e. a shared grid capacity, as in Fig 12, but interactions between the two assets are introduced.

The usable capacity for both consumption and injection are therefore the same as in scenario 2 and given by Eq 12 and Eq 13.

The BESS is still only able to discharge on the grid but has now access to 2 different sources to charge, both the grid and the PV plant.

An important opportunity for BESS when hybridized with a PV plant is the clipping of energy *at the plant's inverter*. The inverter indeed has a maximum capacity that it can handle. When the Direct Current (DC) power input coming from the solar field is greater than this maximum capacity, the Alternative Current (AC) power output is capped to the maximum of the inverter and the excess DC power is lost. This happens only on particularly sunny days, mainly in summer, as shown for example in Fig 14. With the addition of a storage system connected to the solar field, this excess can be directed to the BESS to charge it at low cost or for free. These situations occur when the solar field is oversized compared to the inverter. This is often a voluntary decision, allowing the plant to deliver nominal power for longer periods of time and therefore generating more revenues. Solar plants developers fix the DC to AC ratio, i.e. the oversizing factor, as a balance between additional CAPEX for the larger solar field and extended revenues from energy production.

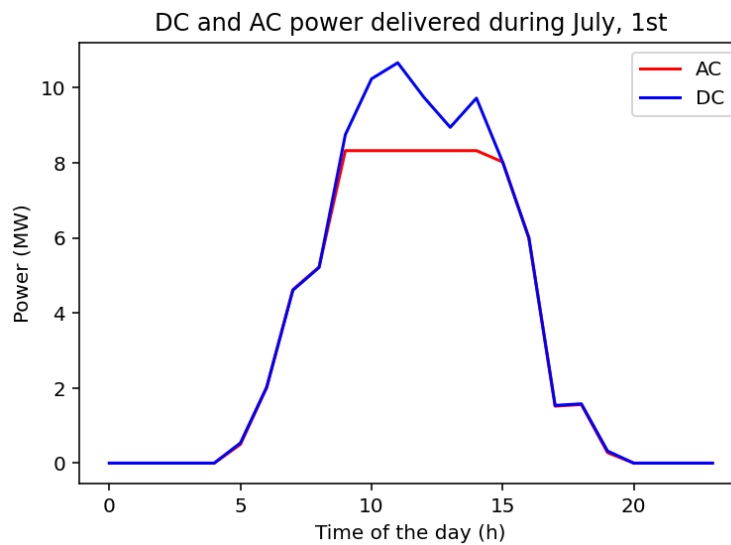


Fig 14: Example of inverter clipping on a summer day for a 8MW PV plant and a DC/AC ratio of 1.5

The Table 4 below summarizes the key characteristics from all 3 scenarios:

Table 4: Grid-related characteristics of scenarios

Characteristics			Scenario 1	Scenario 2	Scenario 3
Assigned grid connection	Injection	PV	$P_{PV, nom}$	Shared	Shared
		BESS	$C_{Grid, inj} - P_{PV, nom}$	$C_{Grid, inj}$	$C_{Grid, inj}$
	Consumption	PV	0	Shared	Shared
		BESS	$C_{Grid, cons}$	$C_{Grid, cons}$	$C_{Grid, cons}$
DC connection for excess PV			No	No	Yes
Usable capacity for the BESS - Consumption			$\min(C_{BESS}; C_{Grid, cons})$	$\min(C_{BESS}; C_{Grid, cons})$	$\min(C_{BESS}; C_{Grid, cons})$

Usable capacity for the BESS - Injection	$\min(C_{BESS}; C_{Grid, inj} - P_{PV, nom})$	$\min(C_{BESS}; C_{Grid, inj} - P_{PV}(t))$	$\min(C_{BESS}; C_{Grid, inj} - P_{PV}(t))$
--	---	---	---

4.3. Dual-loop optimization

The optimization framework operates on a two-tiered structure. At the outer level, a first optimization loop iterates over the entire battery capacity range, systematically evaluating the operational revenues and costs associated with each capacity. Within each fixed-capacity iteration, an inner optimization process determines the optimal BESS dispatch strategy for the selected market, employing a revenue-maximization objective. The complete dual-stage process is presented on the block diagram below in Fig 15.

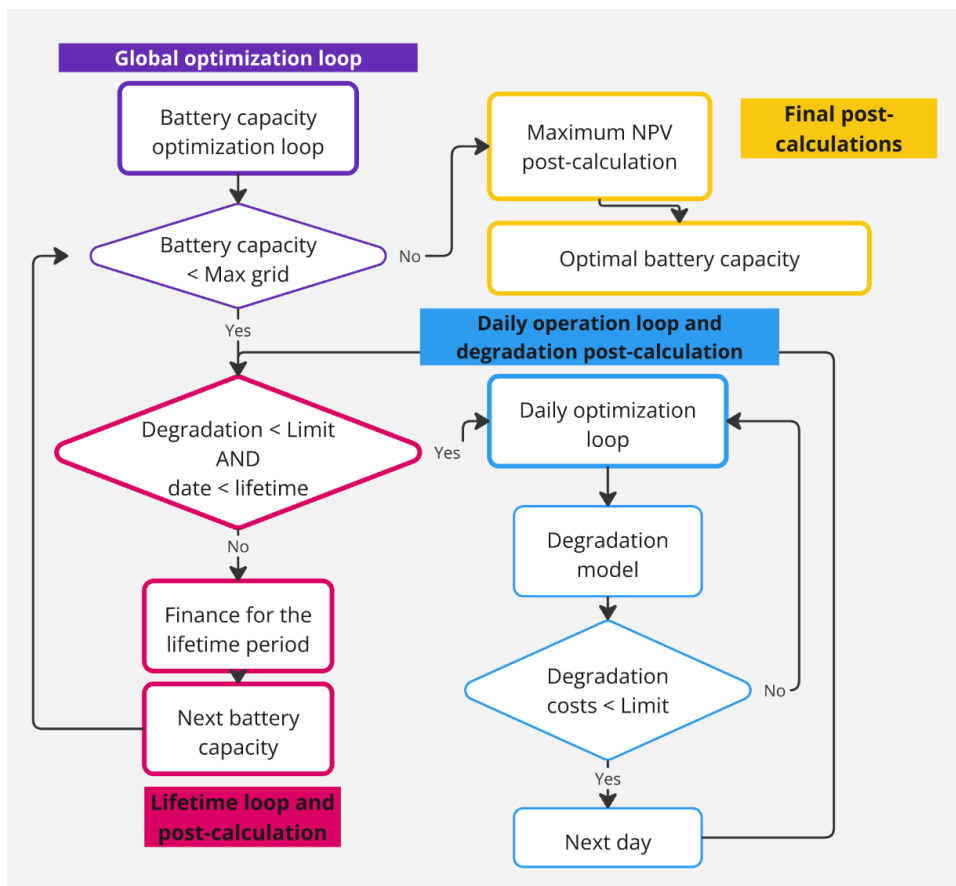


Fig 15: Block diagram of the dual-stage optimization

This section first describes the two optimization stages: the battery capacity optimization stage, and then the daily operation optimization for both spot and FCR-D markets, with consideration of a multi-stage degradation model. Then, the financial and economic parameters used to assess the performance of the BESS are presented. Lastly, the case study chosen for the application of this work is detailed.

4.3.1. Battery capacity loop

The outer-loop is run on the BESS capacity. Given the lower and upper bounds to compute and the step, the whole range of values for the BESS capacity is generated.

For every capacity in this range, the operation is optimized daily until the end of life of the battery, after which the economic assessment of the project over its lifetime is done.

The end of life of the BESS can happen following two different events:

- A. The degradation of the battery has reached its fixed maximum value
- B. The BESS has been operating for its whole given lifetime

Both these parameters are given as inputs. The maximum degradation level is indeed set because the faded capacity heavily impacts the performance of the BESS. A typical value for this maximum is 0.4, which means that the battery has lost 40% of its initial capacity. This value will be implemented as a reference in the model, but the value can be chosen freely as an input. Past this degradation level, the battery is unusable anymore for large-scale storage applications. Second life uses can be considered and are the topic of numerous studies, but this will not be reviewed in this work. On the other hand, a lifetime in years is fixed, whatever the degradation by this time.

4.3.2. Daily operation

Within a fixed battery iteration of the outer loop, the daily operation of the BESS is optimized until it reaches its end of life. In this section are first described the optimization problems for the two operation modes (arbitrage and FCR-D participation) are presented successively. Then, degradation is described with a multi-stage degradation model.

4.3.2.1. Arbitrage on the spot market

The aim of arbitrage is to benefit from price fluctuations over a day to buy energy and charge when prices are low and sell it back by discharging when prices climb again.

Based on the prices and the usable capacity of the BESS, the precise strategy will evolve from one day to another, therefore, to maximize revenues of this operation, an optimization problem can be formulated and is described further. This optimization problem is solved daily to ensure that the maximum revenues are harnessed.

The input parameters and the problem's variables are presented respectively in Table 4 and Table 5.

Table 4: Input parameters for the arbitrage optimization problem

Input Parameters	Symbol	Unit
Time resolution	Δt	h
Spot price per timeslot t	$p_{spot}(t)$	€/MWh
Charging efficiency	η_{ch}	-
Discharging efficiency	η_{dis}	-
Battery capacity	C_{BESS}	MW

Energy storage of the BESS	E_{BESS}	MWh
Usable capacity in injection per timeslot t	$C_{usable,inj}(t)$	MW
Usable capacity in consumption per timeslot t	$C_{usable,cons}(t)$	MW
Clipped PV input (only in scenario 3, otherwise always equal to 0)	$P_{clip}(t)$	MW

Table 5: Variables for the arbitrage optimization problem

Variable	Symbol	Lower bound	Upper bound
Total charging power during timeslot t	$P_{ch,tot}(t)$	0	C_{BESS}
Charging power from PV clipping during timeslot t	$P_{ch,pv}(t)$	0	C_{BESS}
Charging power from the grid during timeslot t	$P_{ch,grid}(t)$	0	C_{BESS}
Discharging power during timeslot t	$P_{dis}(t)$	0	C_{BESS}
Stored energy at the beginning of timeslot t	$E_{st}(t)$	$0.05 \cdot E_{BESS}$	$0.95 \cdot E_{BESS}$
Charging activation state (binary)	$\alpha_{ch}(t)$	0	1
Discharging activation state (binary)	$\alpha_{dis}(t)$	0	1

Objective function

$$\max(\sum_t p_{spot}(t) \cdot (P_{dis}(t) - P_{ch,grid}(t)))$$

Eq 14

Constraints

- The charge must be kept within the usable capacity range:

$$P_{ch,tot}(t) < \alpha_{ch}(t) \cdot C_{usable,cons}(t)$$

Eq 15

- The discharge must be kept within the usable capacity range:

$$P_{dis}(t) < \alpha_{dis}(t) \cdot C_{usable,inj}(t)$$

Eq 16

- The battery cannot both charge and discharge during a single timeslot t:

$$\alpha_{ch}(t) \cdot \alpha_{dis}(t) = 0$$

Eq 17

- The total charge is the sum of the charges from the grid and from the PV plant:

$$P_{ch,tot}(t) = P_{ch,grid}(t) + P_{ch,pv}(t)$$

Eq 18

- The current energy stored in the battery must be updated:

$$E_{st}(t+1) = E_{st}(t) + \eta_{ch} \cdot P_{ch,tot}(t) \cdot \Delta t - \frac{P_{dis}(t)}{\eta_{dis}} \cdot \Delta t$$

Eq 19

Additional constraints

- In Scenario 3, the charge from the PV excess is limited by the available PV input:

$$P_{ch,pv}(t) < P_{clip}(t)$$

Eq 20

- If a maximum number of cycles N_{cycles} is introduced as an input, it must be constrained. A full cycle is composed of a charge and a discharge:

$$\sum_t (\alpha_{ch}(t) + \alpha_{dis}(t)) < 2 \cdot N_{cycles}$$

Eq 21

4.3.2.2. FCR-D participation

When participating in the FCR-D market, the BESS must reserve part or all its capacity and is remunerated for it. Depending on the country of implementation, the participation can be either symmetrical or asymmetrical, as mentioned in 4.2.2.2. Frequency Containment Reserve - Disturbance (FCR-D).

An optimization problem can be established to maximize the revenues through bidding. The input parameters are all the same as in arbitrage previously presented in Table 4: Input parameters for the arbitrage optimization problem, except for two extra inputs: the FCR-D Up and Down clearing prices for each time slot t , respectively $p_{Up}(t)$ and $p_{Down}(t)$.

The FCR-D participation problem's variables are presented in Table 6:

Table 6: Variables for the FCR-D participation optimization problem

Variable	Symbol	Lower bound	Upper bound
Capacity bid for Up regulation during timeslot t	$C_{Up}(t)$	0	C_{BESS}
Capacity bid for Down regulation during timeslot t	$C_{Down}(t)$	0	C_{BESS}
Charging power from the grid during timeslot t	$P_{ch,grid}(t)$	0	C_{BESS}
Discharging power during timeslot t	$P_{dis}(t)$	0	C_{BESS}

Stored energy at the beginning of timeslot t	$E_{St}(t)$	$0.05 \cdot E_{BESS}$	$0.95 \cdot E_{BESS}$
--	-------------	-----------------------	-----------------------

Objective Function

The objective is to maximize revenues, mostly related to reserved capacity remuneration but also from extra incomes on the spot market by selling the excess energy from PV in Scenario 3.

$$\max(\sum_t [p_{Up}(t) \cdot C_{Up}(t) + p_{Down}(t) \cdot C_{Down}(t) + p_{spot}(t) \cdot \eta_{dis} \cdot P_{dis}(t)]) \quad Eq 22$$

Constraints

- The Up and Down bids are limited by the usable capacity respectively in injection and consumption:

$$C_{Up}(t) < C_{usable,inj}(t) - P_{dis}(t) \quad Eq 23$$

$$C_{Down}(t) < C_{usable,cons}(t) \quad Eq 24$$

- The cumulated bid must stay within the technical capacity of the BESS:

$$C_{Up}(t) + C_{Down}(t) < C_{BESS} \quad Eq 25$$

Additional constraints

- When the participation is symmetrical, the Up and Down bids must be equal:

$$C_{Up}(t) = C_{Down}(t) \quad Eq 26$$

- In Scenario 3, excess PV generation can be sold on the spot market:

$$P_{dis}(t) < \eta_{ch} \cdot P_{clip}(t) \quad Eq 27$$

The State of Charge of the battery is assumed to be on average at 50% the whole day in symmetrical markets and at $SoC(t) = \frac{C_{Up}(t)}{C_{BESS}}$ for time slot t in asymmetrical markets. As activation orders are sometimes received, small charges and discharges can occur. Historical data however show that activations of the FCR-D reserve are not systematic every hour and the activated capacity, either Up or Down, is usually smaller than 5% of the reserved capacity, except during rare large imbalances. In addition, activations occur in both directions in the course of the day, making the balance between selling and buying these small amounts break even at the end of the day.

4.3.2.4. Degradation

Degradation is an important part of the model as it will affect the battery capacity over time

and consequently, the revenues. Whereas some models implement basic linear degradation over the lifetime, a deeper understanding and application of degradation models helps have a more precise idea of the battery future. Articles have already studied the impact of degradation on BESS operation and how to adapt to it. As an example, in [40], degradation is presented for operation on Swedish electricity markets and ancillary services, using non-linear models. [41] goes further on the topic by implementing a multi-stage optimization model for degradation. Based on the first optimized daily operation of the BESS, degradation is turned into degradation costs which are, in turn, converted into a function of the SOC. Further optimizations are run considering these degradation costs in the revenues objective function, until degradation costs reach a stable value from one loop to another. This operates the BESS in the optimal way to reduce degradation costs. Therefore, the system can choose not to charge nor discharge if prices are not worth the related degradation.

The degradation in the tool is implemented according to this method and additions from [40] and is shortly described below.

Non-linear degradation L is applied through a linear degradation rate f_d in a model involving it and initial solid electrolyte interface (SEI) parameters as follows in Eq 28:

$$L = 1 - \alpha_{SEI} \cdot e^{-\beta_{SEI} \cdot f_d} - (1 - \alpha_{SEI}) \cdot e^{-f_d}$$

Eq 28

$$\text{With } \alpha_{SEI} = 0.550 \text{ and } \beta_{SEI} = 128.2$$

The degradation L is a direct image of the faded capacity, illustrating the share of the initial capacity that disappeared. The initial degradation L_0 is then 0 and a degradation of $L = 0.25$ means that the BESS lost 25% of its capacity.

The linear degradation rate f_d is modeled as a combination of two separate factors, calendar and cycling aging. Calendar aging f_{cal} is a passive degradation due to the electrochemical reactions happening in the battery over its lifetime, when staying still in a stationary state. The degradation is especially fast in the beginning, as the SEI forms consuming active components. It depends on the stationary time, the ambient temperature and the average state of charge over the period, each parameter inducing a stress factor

Cycling aging f_{cyc} is an active degradation due to the charging-discharging cycles during the battery operation. Each cycle slightly degrades the battery with different impacts based on the average state of charge over the cycle, the cell temperature, the depth of discharge and the type of cycle (full or partial).

On the spot market, cycles are identified by a Rain Counting Algorithm (RCA) as explained and used in [40]. The algorithm takes the hourly state of charge and identifies each cycle with its associated depth of discharge, type and average state of charge.

On the FCR market, cycles are not directly implemented. In fact, as the delivered energy is not remunerated only the standing stationary reserve is considered as revenue. In the event of an activation, the asset must provide a service proportional to the frequency change. As mentioned previously in 4.2.2.2. Frequency Containment Reserve - Disturbance (FCR-D), activations in FCR-D are not systematic and quite small, therefore, there is very little delivery

of energy and change in the state of charge. It can be considered that such activations do not add any degradation to the battery overall.

A multi-stage degradation optimization is run after the first daily operation optimization. The goal is to maximize the revenues, while minimizing the degradation costs of the associated cycles. The first loop is run without consideration of degradation costs. The state of charge and cycles are then converted into degradation and degradation costs in the following Eq 29.

$$cost_{degrad}(t) = \frac{L(t) - L(t-1)}{L_{max}} \cdot CAPEX$$

Eq 29

To take these costs into consideration in the next iteration, they must be related to the *problem's variables*. These variables are the activation signals for charge and discharge, images of the energy changes and cycle degradation, and the state of charge, reflecting the stationary degradation. Costs are then converted into a linear function of these variables as follows in Eq 30.

$$cost_{degrad}(t) = a \cdot (\alpha_{ch}(t) + \alpha_{dis}(t)) + b \cdot SoC(t)$$

Eq 30

The values of the linear constants are dependent on the battery capacity on that loop, as the costs are defined on the CAPEX. The constant a is the cost degradation associated with a partial cycle of 90% depth of charge and 50% average state of charge. The constant b is the cost degradation associated with a calendar stationary degradation during a time period Δt and with an average state of charge of 50%. Values of these constants are given in Table 7

Table 7: Constant parameters for degradation costs linearization

Linear constant	Value	Unit
a	$3.03 \cdot 10^{-6} \cdot CAPEX$	€
b	$4.89 \cdot 10^{-6} \cdot CAPEX$	€

Further loops are run with an adapted objective function in Eq 31:

$$\max\left(\sum_t [p_{spot}(t) \cdot (P_{dis}(t) - P_{ch,grid}(t)) - cost_{degrad}(t)]\right)$$

Eq 31

After every loop, the difference between the degradation costs of the loop and the previous one is calculated. Once convergence is reached, i.e. the difference is less than 1%, the operation for the day is considered complete and the algorithm moves forward to the next one. If convergence is not reached, another updated daily optimization happens.

After each day, both calendar and cyclic degradations are applied based on the said operation. The corresponding degraded capacity is the new capacity for the next day.

4.3.3. Economic assessment

The optimal battery capacity out of the whole range is determined through a maximization of the Net Present Value (NPV) of the BESS all over its lifetime.

To perform this calculation, some economic parameters are used:

The yearly cashflow is the key parameter for the further calculation of the NPV. It refers to the total amount of money generated by the BESS over the year, accounting for all incomes and expenses.

$$CF_{year} = \sum incomes - \sum expenses$$

Eq 32

In this study, incomes are the direct profits of the operation of the BESS on the energy markets. The operation is optimized daily to maximize these revenues, and the optimization process is described earlier in 4.3.2. Daily operation.

The expenses, on the other hand, are of different types:

Capital expenditure

During the construction phase, the expenses based on the CAPEX are split equally over the years. The CAPEX is divided into two parts: a fixed CAPEX independent on the battery size $CAPEX_{fixed}$ and a variable CAPEX dependent on the battery size $CAPEX_{Var}$. The total CAPEX is therefore given by Eq 33:

$$CAPEX_{total} = CAPEX_{fixed} + CAPEX_{Var} \cdot C_{BESS}$$

Eq 33

Operation expenses

The operation expenses are divided into the same categories: fixed OPEX independent on the battery size $OPEX_{fixed}$ and variable OPEX dependent on the battery size (Grid connection costs, maintenance...) $OPEX_{Var}$. As OPEX are paid in the operating years of the BESS, inflation must be applied to them:

$$OPEX_{year\ n} = (OPEX_{fixed} + OPEX_{Var} \cdot C_{BESS}) \cdot (1 + i)^{n_{construction} + n}$$

Eq 34

Where:

- C_{BESS} is the installed BESS capacity in MW
- i is the inflation rate
- $n_{construction}$ is the duration of the construction phase in years
- n is the current year of operation

Tax expenses

The company owning the BESS and operating it must pay taxes on the incomes and costs related to it:

$$Taxes_{year\ n} = r_{tax} \cdot (Income_{year\ n} - OPEX_{year\ n} - r_{depreciation} \cdot n)$$

Eq 35

Where:

- r_{tax} is the tax rate
- $r_{depreciation}$ is the depreciation rate of the BESS, i.e. the value the asset loses every year

Net Present Value (NPV)

The economic factor used to compare and estimate the best opportunity is the Net Present Value (NPV), whose formula is given below:

$$NPV = \sum_{n=0}^{n_{construction}+n_{lifetime}} CF(n) \cdot \frac{1}{(1+r)^n}$$

Eq 36

Where:

- $n_{lifetime}$ is the operating lifetime of the battery in years
- r is the discount rate, i.e. the required rate of return
For companies, a good indicator of this rate is the Weighted Average Cost of Capital (WACC), corresponding to the rate required to finance its assets.

Internal Rate of Return (IRR)

Following the NPV, another economic indicator is computed, the Internal Rate of Return (IRR). It is the rate of return that will make the project exactly balanced, with an NPV equal to 0.

$$NPV = 0 = \sum_{n=0}^{n_{construction}+n_{lifetime}} CF(n) \cdot \frac{1}{(1+IRR)^n}$$

Eq 37

To make the project cost-effective, the IRR must be higher than the WACC.

4.3.4. Post-calculations

Once the battery has reached its end of life, either from degradation limit or from life expectancy, the optimal battery size is evaluated. The chosen criteria is the NPV, making the optimal size the size that will generate the most money for the developer.

The associated yearly cash flow and internal rate of return are extracted from the economic calculations and results are available. Based on the data detailed in 4.4 Case study, the results of the sizing process are presented in 5. Results.

4.4 Case study

The chosen case study for the application of the tool is the PV power plant of Hallstahammar,

Västmanland in Sweden.

The choice of Sweden has been motivated by several factors, such as its high renewable energy penetration, especially wind and hydropower, strong seasonal solar variability, and supportive policies and market changes. The Swedish electricity mix is indeed mostly based on renewable sources, and with a national goal of 100% renewable electricity by 2040, it tends to increase. To reach this target, large-scale PV installations are growing quickly, making the Swedish electricity generation even more intermittent, leading to a need for energy balance and storage. On the other hand, Sweden observes important seasonal variations in terms of sunlight, long summer daylight hours causing surplus generation and short winter days reducing solar output, making energy storage essential for balancing supply and demand. The Swedish electricity markets will furthermore soon switch from an hourly resolution for market prices to a 15-minute resolution.

The model used for the battery is from CATL large-scale battery model, one of the leaders in battery manufacturing in the world. The battery is a Li-ion type, specifically a Lithium iron phosphate (LFP) battery type, having LFP as cathode material and graphite as anode material. The battery considered has a C rating of 1, corresponding to an energy stored equivalent to 1h of full power capacity discharge. The battery can handle about 12,000 cycles in its lifetime, corresponding to about 15 years of operation with 2 cycles a day. The battery is also considered to be placed in containers to isolate from exterior conditions and with a Heating, Ventilation, Air Conditioning system (HVAC) to regulate the internal temperature. [57]

The data used for the application of the tool to the case study are presented in Table 8 and extracted from [59] and from internal data from Flower [60]:

Table 8: Input data related to the chosen case study [59][60]

General and site-specific data		Economic data		
Country	Sweden	CAPEX	Fixed	1.0 M€
Latitude	59.59003° N		Variable	600k€/MW
Longitude	16.22582° E	OPEX	Fixed	3.3 k€/year
Grid Connection capacity	45 MW		Variable	40k€/MW/year
PV nominal Power	10 MWp	WACC		25%
AC/DC ratio	1.5	Depreciation time		15 years
BESS lifetime	15 years	Inflation rate		2%
Commissioning year	2025	Tax rate		20.6%

4.4.1. PV forecasts

Using the Python library PVlib which is linked by I/O tools [61] to the PVGIS database of solar irradiation from the European Commission [49], weather profiles using the TMY method have

been extracted, allowing then for the creation of PV generation profiles. Examples of a summer and winter days are presented in Fig 16.

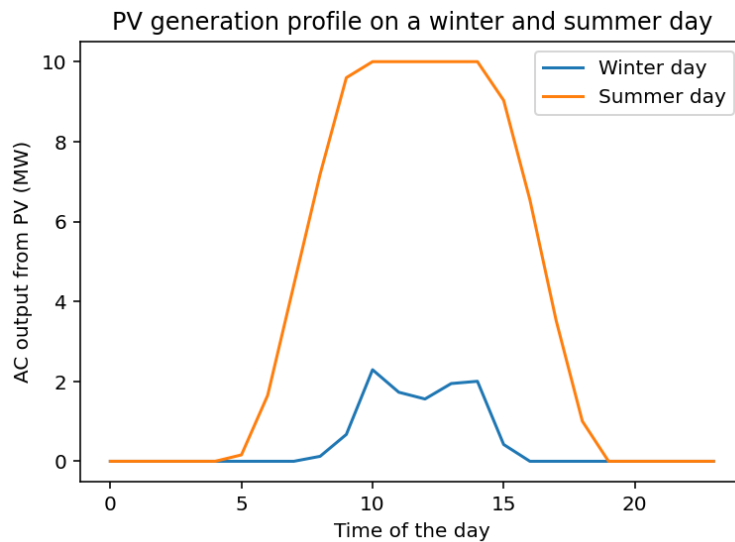


Fig 16: PV generation profiles on a winter and a summer day

4.4.2. Price forecasts

The data for long-term prices estimations were exported from long-term market analyses from Svenska Kraftnät. Spot market trends are from a 2050 evolution of the Swedish grid and market [62] and the FCR-D estimations are from an analysis focusing on balancing market towards 2030 and 2050 [63]. The global trends used to build profiles are presented in Fig 17.

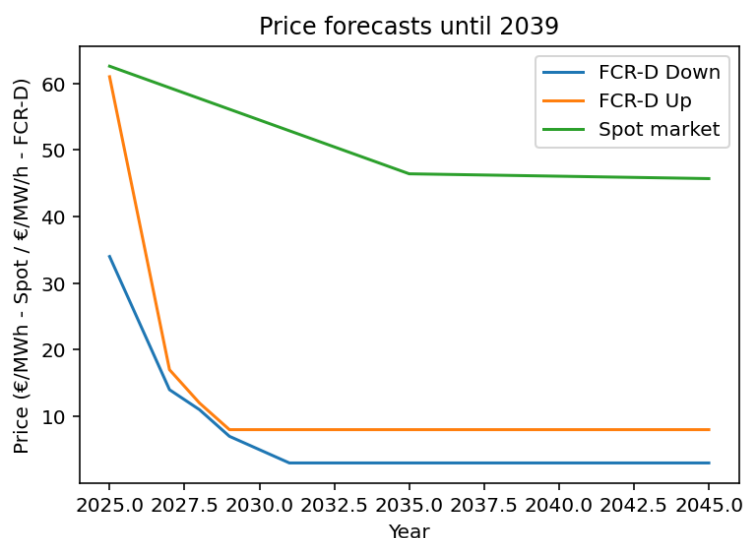


Fig 17: Long-term price trends for Spot market, FCR-D Up and Down

FCR-D prices are expected to fall drastically in the coming years, reaching a low stable price. Spot market prices in Sweden are expected to decrease on average as the grid is developed stronger, increasing Sweden autonomy and resilience.

The historical data for the phasing building were imported from the European Network of Transmission Systems Operators for Electricity (ENTSO-E) transparency platform [64] for Spot market prices and from the platform Mimer from the Swedish grid, Svenska Kraftnät, for

the FCR-D Up and Down prices [65].

5. Results

This chapter will focus on the results of the tool for all scenarios and markets, discussing the differences and similarities. For both the spot and FCR-D market, the results will be presented from an economic point of view and from a degradation perspective as well.

Given the previous data from 4.4 Case study and the forecasts built in the previous parts 4.4.1. PV forecasts and 4.4.2. Price forecasts, the tool has been run under all 6 configurations, all three scenarios for both market participation (arbitrage and FCR-D). This part aims at exposing results under this situation and understanding them in the context of co-location.

Using the grid data presented previously, the grid capacity allowances in all scenarios are described in Table 9.

Table 9: Grid capacity in both directions for the PV plant and the BESS under each scenario

Scenarios		Scenario 1	Scenario 2	Scenario 3
Allowed capacity injection for	PV	10 MW	45 MW	45 MW
	BESS	35 MW		
Allowed capacity consumption for	PV	0 MW	45 MW	45 MW
	BESS	45 MW		

5.1. Arbitrage on the spot market

The global trend in arbitrage is a fast and linear decrease in NPV over tested battery capacities. This large loss when battery capacity increases can be explained by detailing the incomes and costs. With an average of 2 cycles a day on the spot market and an average *range of volatility for prices of 50€/MWh, the average daily income is about 100€ per MW of installed capacity (given a 1h storage assumption). This represents a yearly revenue of approximately 36.5k€/MW installed. On the other hand, a value of 40.3k€/MW has been considered for the OPEX in this application. Those two values show a clear net loss every year, without consideration of the initial CAPEX. Details for every scenario are given in the different sections below, followed by a consideration of the degradation in arbitrage.*

Scenario 1

Under this scenario, the optimal capacity for the battery *is 5 MW. However, this “optimal” solution is the lower bound of the range of tested battery capacities. This means that this configuration is still not financially viable but with the least financial loss, as this indicator is*

linear with installed capacity, as seen in Fig 18.

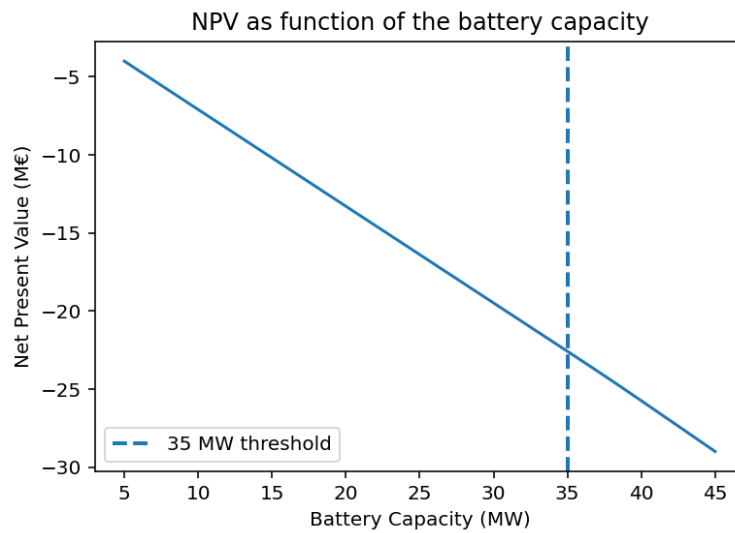


Fig 18: NPV per battery capacity - Spot Market - Scenario 1

Looking solely at the incomes on Fig 19 helps to better understand the phenomena. The graph on this figure can be split into two parts. The threshold dividing is placed at 38.9 MW. This corresponds to the installed capacity for which the maximum injection on the grid is reached. This maximum is not 35 MW as one could expect because of the fixed depth of discharge of 90%, implemented to limit full charges and charges, degrading the battery. The threshold is then $C_{threshold} = \frac{C_{grid,inj}}{0.9} = 38.9 MW$.

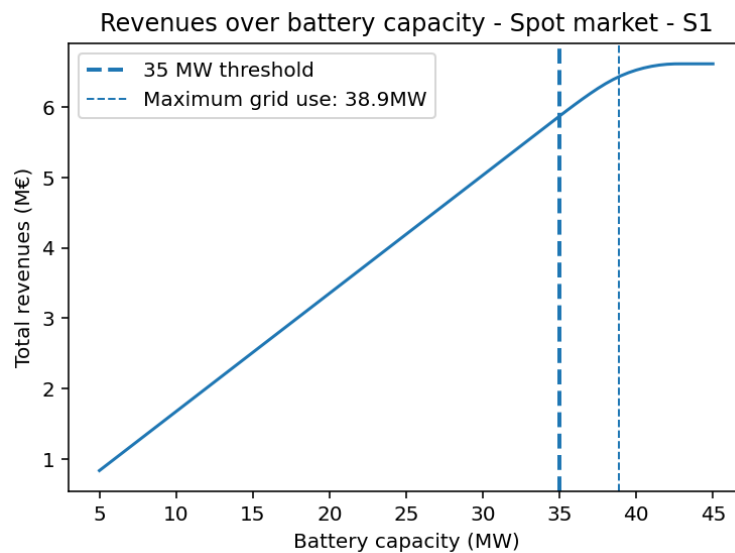


Fig 19: Income per battery capacity - Spot Market - Scenario 1

The first segment, from 5 to 38.9 MW capacity, is a linear regression, where income is proportional to the installed capacity. This is coherent with the fact that the PV adds no constraints to the BESS before it reaches a capacity corresponding to the maximum injection possible.

The second part, past 38.9 MW capacity is a horizontal line, meaning a constant income from the threshold up to the last tested capacity of 45 MW. Once the threshold has been reached, the battery cannot inject anymore and therefore limits the earnings, stabilizing them to the same amount, while battery-related costs still increase.

Scenario 2

In this scenario, the optimal capacity is again 5MW, the lower bound, as seen in Fig 20 for the reasons explained earlier.

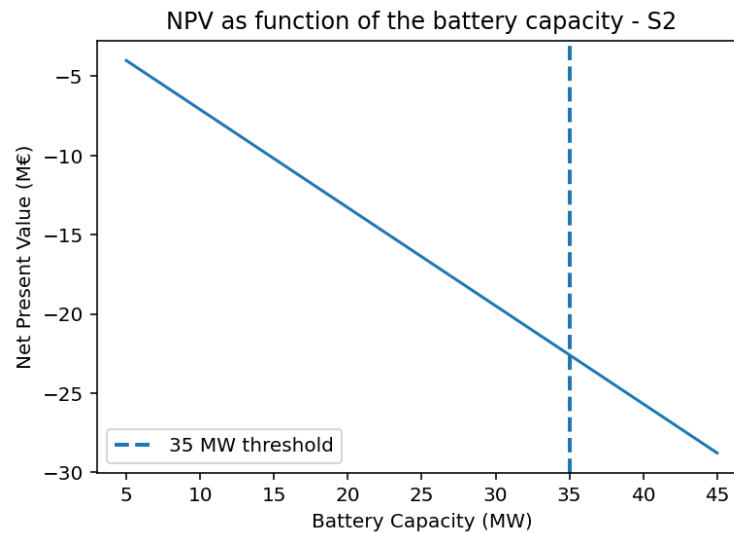


Fig 20: NPV per battery capacity - Spot Market - Scenario 2

However, the graph of income in Fig 21 below shows a different evolution with installed battery capacity. The graph is no longer split into two different parts, showing a linear relationship all the way to the maximum tested capacity. This difference in the higher values of capacity can be explained by the connection configuration. Where the income slope was lower after the threshold in Scenario 1, it is now the same, meaning that the BESS can use its whole capacity even with the PV injection limitation. In fact, the PV power is injected on the grid only during daytime, when prices are usually low. On the other hand, in the typical daily price profile the prices are high early in the morning just before the PV starts producing and in the early evening, right after the PV stops its generation. This implies that at interesting times for BESS arbitrage, the PV is not limiting. Therefore, even with a full capacity of 45MW, the PV can use the whole range.

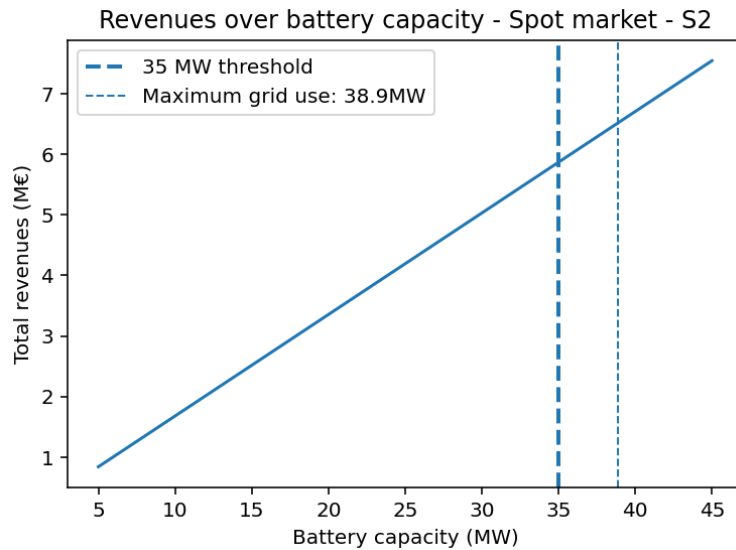


Fig 21: Income per battery capacity - Spot Market - Scenario 2

Scenario 3

This scenario has the same grid connection configuration as scenario 2, i.e. PV and BESS sharing 45MW of grid capacity.

The same trend as in previous scenarios for arbitrage can be observed on Fig 22: a linear relationship with a negative slope. The optimal size in this scenario is 5 MW, limiting the negative NPV of the whole system.

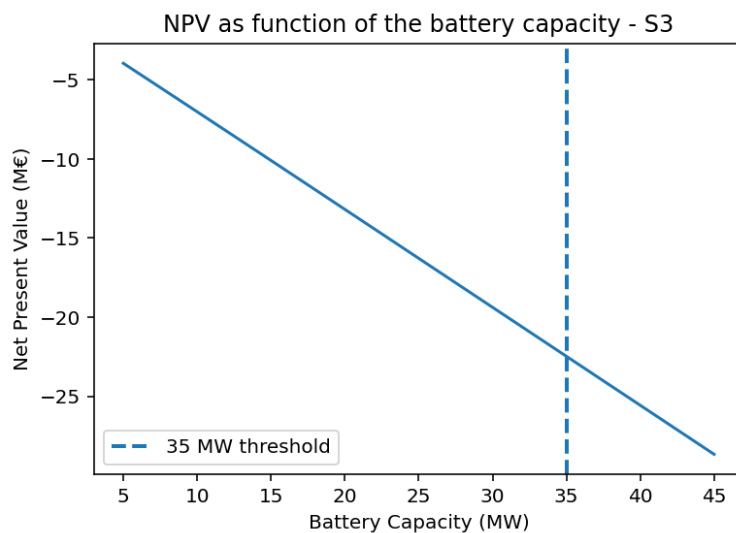


Fig 22: NPV per battery capacity - Spot Market - Scenario 3

The income curve is slightly different here, as seen in Fig 23. The overall shape is almost the same, however, it has been shifted up. Compared to scenario 2, the revenues are higher for all battery capacities, thanks to the use of the excess PV to charge. This allowed the BESS to charge partly for free instead of buying on the spot market. The added revenue related to this excess PV is a fixed quantity, independent of the battery capacity since it is linked to the design

of the PV plant. This explains the same slope for income increase but a shift upwards.

At the very beginning of the curve, a different evolution can be noticed, with a slightly larger slope. This is because of the limited size of the battery, smaller than the maximum excess PV power of about 5MW. The BESS is then able to charge fully from excess when it hits, greatly decreasing the charging costs.

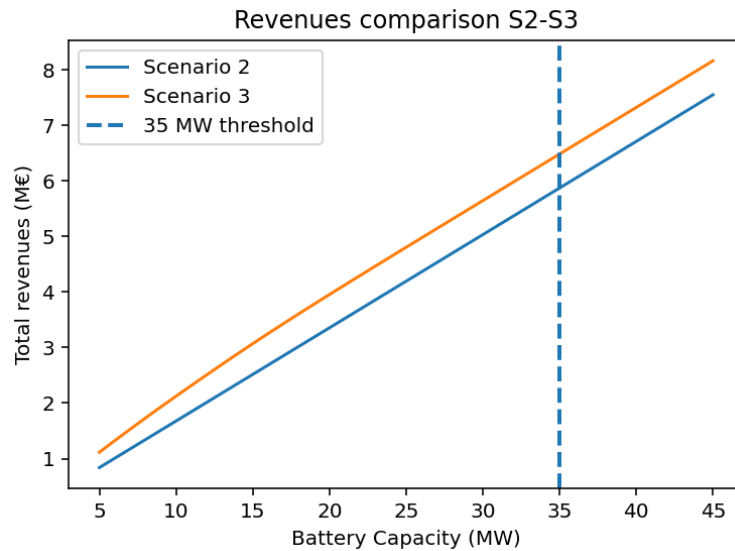


Fig 23: Comparison of incomes per battery capacity - Spot Market - Scenarios 2 and 3

Degradation in arbitrage

The degradation of the battery is primordial to consider in arbitrage. The cycles are indeed heavily impacting the health of the battery. The degradation under all three scenarios is presented in Fig 24.

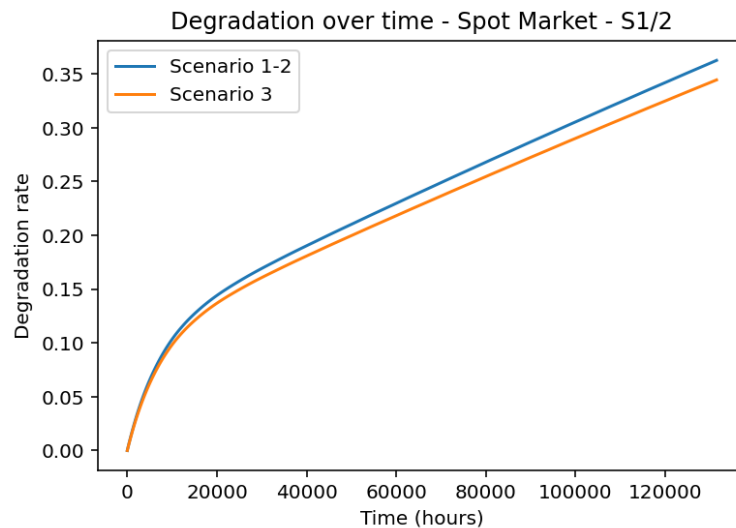


Fig 24: Degradation over lifetime for arbitrage in scenarios 1, 2 and 3 for a 35 MW battery

Under this operation, the end of life of the battery is reached after a period of 15 years, the

maximum lifetime set as input. The degradation after this time is indeed smaller than 40%, the maximum degradation level set as input.

It can further be observed that the degradation is the same for scenarios 1 and 2, as they are operating the same: full charges (respectively discharges) between the two extremal states of charge, therefore the maximum depth of charge when prices are low (resp. high). This operation leads to a degradation of 36.2% at the end of life. Full charges or discharges over a limited period, such as a single hour, generate a lot of heat in the system, which induces an acceleration of the degradation.

The third scenario, however, shows a slightly lower degradation at the end of lifetime, with 35.7% of capacity fading. This small difference can be explained by the excess PV power used here. In fact, the excess PV is not generated all at once during a single hour. This allows the BESS to charge several times with a small depth. These slower and smaller charging cycles create less degradation than one full cycle happening during a single hour. This phenomenon does not happen often, as excess generation occurs only 7% of the time, during peak sunlight in summer days.

5.2. FCR-D participation

The second type of market consideration is participation in an ancillary service: FCR-D. In Sweden, this service is asymmetrical, meaning that the bids in Up and Down can be differentiated.

As opposed to arbitrage, participation in FCR-D ensures a stable revenue stream every time slot. This is reflected in the results in all three scenarios, with positive NPV and revenues increasing with the size of the battery. A detailed analysis of the results for each scenario is given below.

Scenario 1

The optimal size in this case is 35MW. It is clear on Fig 25, showing the highest NPV of all. This figure can be divided into two parts with different evolutions. The threshold between these is located at a BESS capacity of 35MW, corresponding to the grid limit for the BESS.

On the left, the NPV is directly proportional to the size of the battery. The battery bids its whole capacity, mainly in the Up Reserve as the prices are higher on average. This ensures revenue is proportional to the battery capacity. Once reaching the threshold, the maximum for injection has been reached, therefore, capacity must be bid on the Down service now. The prices being *lower on this market on average, the additional revenues from this don't meet the OPEX, still identical*. Therefore, a decrease in the second part is observed.

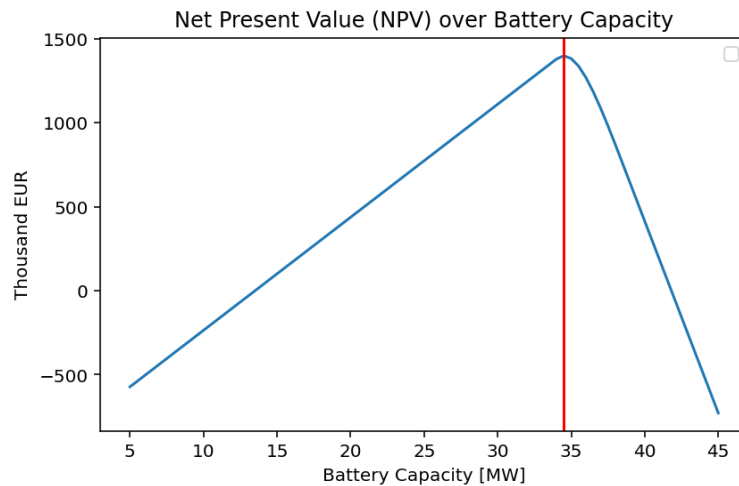


Fig 25: NPV per battery capacity - FCR-D - Scenario 1

Scenario 2

Under this scenario, the optimal battery size is 41.1 MW as seen on Fig 26(a).

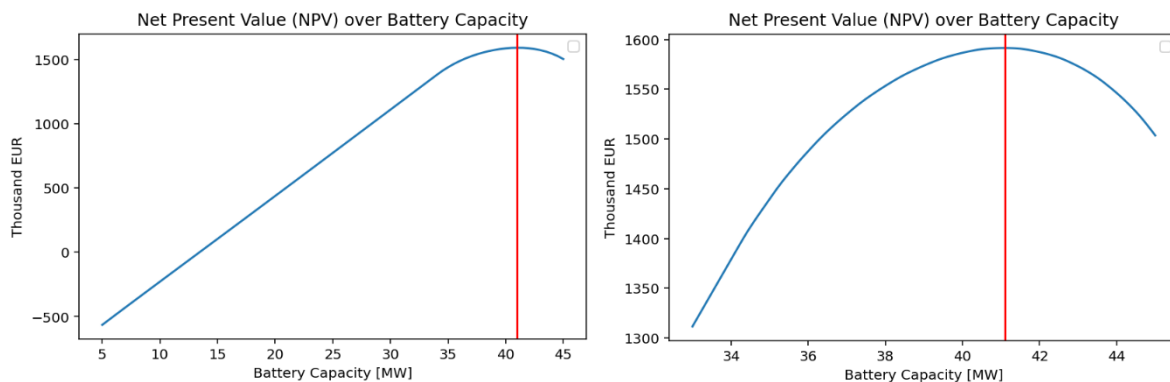


Fig 26 (a)(b): NPV per battery capacity - FCR-D - Scenario 2: Complete range (a) and Zoom (b)

As in all previous cases, a break can be noted at 35MW, dividing a linear regression and another part, in the shape of a parabola. The first part is the same as in scenario 1. The second, however, presents a unique shape shown on Fig 26(b), increasing until a maximum value and then decreasing slowly. This shape is the consequence of the limitations brought by the PV plant. Until 35 MW the BESS can bid in any direction without limitation, allowing it to maximize revenues on the Up market. Between 35 MW and 45MW of BESS size, the PV will progressively apply limitations on the injection for the BESS to operate, forcing it to switch to more frequent Down participation and therefore lowering revenues.

Scenario 3

The optimal battery size in this final case is 41.1 MW again as seen on Fig 27(a), with an NPV of 1.78 M€.

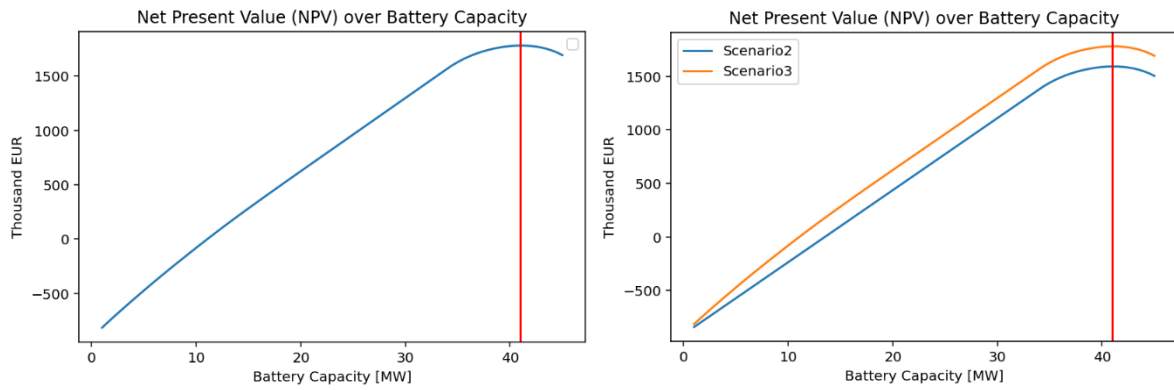


Fig 27 (a)(b): NPV per battery capacity - FCR-D - Scenario 3 (a) and Scenario 2-3 comparison (b)

The same situation as for Scenario 3 in arbitrage occurs here. The curve is once again the same as in Scenario 2 but shifted upwards, as seen in Fig 27(b). Whereas in arbitrage, the use of excess PV power allows for a reduction in costs related to the purchase of energy, in this scenario it allows for a net extra revenue. This excess is sold on the spot market while bidding mainly on the FCR-D Up. This extra is again a fixed amount and is estimated to be 1.08 M€ over a 15-year lifetime.

Degradation in FCR-D participation

The degradation in FCR-D operation is mainly due to calendar aging. The degradation profiles for the 3 scenarios are given in Fig 28.

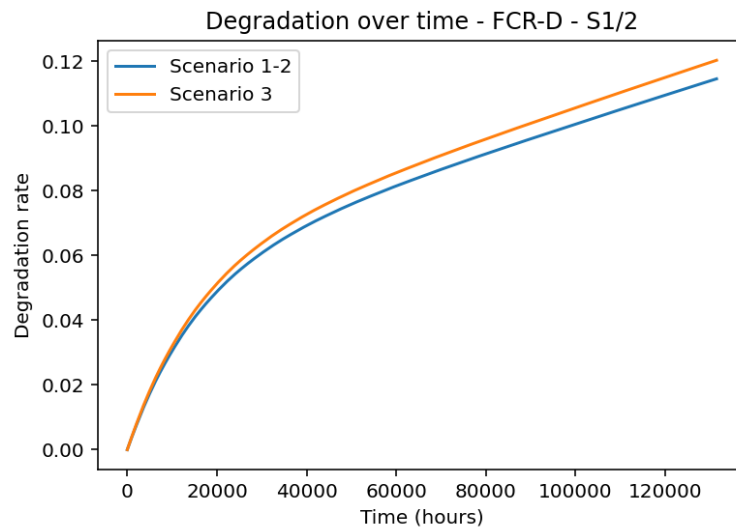


Fig 28: Degradation over lifetime for FCR-D in scenarios 1, 2 and 3 for a 35 MW battery

The end of life is reached after 15 years, the limit for operation implemented as input, meaning that the degradation level after this period of time has not reached the maximum of 40% set up initially.

The battery reaches a degradation state of 11.4% in scenarios 1 and 2, whereas in scenario 3, it reaches 11.9%. This difference is due to the extra partial cycles that are operated when charging and discharging the excess PV power. Repeated small cycles add up to this

difference.

5.3. Summary of results

The Table 10 below sums up the results of optimal capacities, NPV and incomes for all 6 cases.

Table 10: Results for all configurations (2 markets, 3 scenarios)

Operation	Arbitrage on Spot Market			FCR-D participation		
	Scenario 1	Scenario 2	Scenario 3	Scenario 1	Scenario 2	Scenario 3
Optimal capacity (MW)	5	5	5	35	41.1	41.1
NPV (M€)	-4.01	-4.01	-3.95	1.39	1.60	1.78
Income (M€)	0.83	0.83	1.15	76	92.2	93.3
Extra income from excess PV (M€)	-	-	0.316	-	-	1.08

The study aimed to achieve two key objectives: to evaluate the economic viability of battery storage participation in arbitrage versus FCR-D markets and to determine the optimal BESS capacity for each market configuration in a co-located PV system. The findings indicate that FCR-D participation significantly outperforms arbitrage in terms of profitability, while arbitrage leads to consistent financial losses. In the arbitrage market, the optimal battery size was found to be 5 MW, the lowest tested capacity, as increasing storage size only amplified financial losses due to low price volatility and high operational expenses. Conversely, in the FCR-D market, the optimal battery capacity ranged between 35 MW and 41.1 MW, depending on grid limitations, with revenues increasing with size up to the injection threshold.

In addition to profitability, the degradation analysis highlights key differences in market participation strategies. Arbitrage operations led to a 36.2% capacity fade over the battery lifetime due to high cycling frequency, whereas FCR-D participation resulted in only close to 12% degradation, primarily driven by calendar aging rather than deep discharge cycles. The excess PV power utilization in Scenario 3 slightly reduced degradation in arbitrage and increased revenues in FCR-D, shifting optimal sizing decisions upward. This finding underscores the need for degradation-aware optimization when sizing BESS for different market applications.

From Table 11, it is clear that while arbitrage in the spot market is consistently unprofitable under current market conditions, *FCR-D participation provides a positive NPV (up to €1.78M)* and ensures a stable revenue stream. However, FCR-D prices are subject to future regulatory changes and market saturation risks. On the other hand, if volatility on spot market prices increases, earnings could move accordingly and make arbitrage a viable option. The shift from hourly to 15 minutes resolution in Sweden and in other countries can lead to short-time volatility and create new opportunities. In such cases, additional cycles per day might happen, reducing the overall lifetime of the battery.

A hybrid strategy, combining arbitrage when price spreads increase while prioritizing *FCR-D participation, could enhance profitability and risk resilience. Depending on the user's risk appetite, a combination of split-capacity operation or dynamic switching between markets may be an optimal strategy, ensuring both financial stability and long-term sustainability of the co-located PV-BESS system.*

The results highlighted in this study also align with the existing literature on the topic. Similar studies have for example demonstrated that energy arbitrage profitability is highly dependent on market price volatility and operational costs, with low price differentials making arbitrage financially unsustainable. This trend is observed in the work of Wu et al. [36], which highlights that arbitrage viability is limited by low spreads and transaction costs, reinforcing the conclusion that under current market conditions, arbitrage alone does not justify large-scale battery storage investments. On the other hand, studies such as those by Zhu et al. [20] and Villar et al. [14] highlight the benefits of frequency regulation services in providing stable revenues, which is consistent with the results in this study.

The degradation results are in phase with existing studies as well. In the work from Serres [40], the same degradation trends are observed in arbitrage and in FCR participation. The integration of excess PV power in Scenario 3 also validates the insights from Xu et al. [35]

regarding the role of PV surplus in improving battery economics and extending system lifetime.

6. Limitations and future work

Limitations

FCR-D Activations

This thesis assumes a very limited impact of FCR-D activations, both from the revenues side and the degradation perspective. However, even if the individual impact of an activation is small, the global impact of all of them can deeply change the conclusions. This simplification may impact the accuracy of the results, particularly in assessing the financial viability and operational feasibility of BESS participation in ancillary services.

Assumption of a 1-Hour Battery

The analysis is constrained by the assumption that the battery has a fixed 1-hour duration (i.e., energy-to-power ratio of 1 MWh per MW). In real-world applications, BESS systems come in various configurations, the most common nowadays being 2 or 4 hours, and some experimental projects reaching 8 hours. The optimal duration may depend on multiple factors, including market requirements, revenue stacking opportunities, and degradation considerations. This assumption may limit the generalizability of the findings to different battery configurations.

Challenges in Long-Term Forecasting (Both PV Generation and Market Prices)

Forecasting future PV generation and electricity prices is inherently uncertain. This thesis relies on simplified forecasting approaches based on historical patterns, assuming the same trends for the future. No extreme events are considered for these profiles, even though they could have a great impact on results, either positively or negatively. These assumptions could lead to deviations from actual long-term trends.

Limited to Two Markets

The study is restricted to the analysis of only two electricity markets, arbitrage and FCR-D, which may not capture the full spectrum of market opportunities and challenges that exist globally. Different markets have varying regulatory structures, auction mechanisms, price dynamics, and ancillary service requirements, which may influence the feasibility and profitability of hybrid PV-BESS participation. Considering a larger spectrum of markets can allow for more revenue sources and a higher cost-effectiveness in the end.

Unaddressed aspects

Multi-Market Participation

The study does not explore strategies for simultaneous participation in multiple markets (e.g., combining energy arbitrage with ancillary services). Operating in several markets can help tackle the downsides while taking advantage of strengths. Maximizing the profitability of PV-BESS systems often involves dynamic multi-market strategies, which are not analyzed in this

work.

Deeper Hybridization Between PV and BESS

While the thesis likely considers a PV-BESS hybrid system, it does not investigate more advanced hybridization techniques, such as direct DC coupling, advanced energy management strategies, or integrated inverters. These aspects could further optimize system efficiency, reduce conversion losses, and enhance revenue streams.

Regulatory Framework and Country-Specific Considerations

The study does not provide an in-depth analysis of regulatory frameworks that govern PV-BESS operations in different countries. Regulations on grid connections, market participation, incentives, and energy storage ownership vary widely across jurisdictions and can significantly impact the economic feasibility of hybrid systems. A more detailed regulatory analysis could provide additional insights into barriers and opportunities in specific regions.

Yearly Economic Assessment Limitation

The economic analysis is conducted on a yearly basis, which provides an overall view but lacks precision in capturing seasonal variations. A monthly assessment could offer better insights into how fluctuations in energy prices, PV generation, and market conditions impact financial performance. For example, the PV generation is higher in the summer, putting more limitations on the BESS operation and therefore limiting revenues. For simplicity and feasibility, a yearly approach was chosen.

Future work

Considering these limitations and uncovered aspects, further work on the tool structure and possibilities can be studied.

Three leads for future work emerge:

- Develop the market entries

The completion of the tool to make it able to handle more energy markets and even a multi-market participation would make this work usable on a larger scale.

- Investigate deeper connection and relationships between the PV and the BESS

The relationship between PV and BESS in this work is mainly from a grid perspective. Deeper understanding of the potential hybridization between the two assets can show new strategies to harness energy and revenues.

- Implement regional or country specific regulations and policies

A comprehensive investigation of the national regulations related to market entries, grid connection or development of sustainable energy solutions can help to have more precise results and ideas on the potential of a business case.

7. Sustainability assessment

The development of co-located PV-BESS power plants plays a crucial role in enhancing the sustainability of energy systems by improving grid stability, increasing the share of renewable energy, and optimizing energy market participation. However, sustainability is not only considering impacts on the present-time but also for the future. Therefore, the sustainability assessment of this work described in this chapter is split into two sections. The first one focuses on intra-generational equity, reviewing the impacts on the present generation, while the second part handles the inter-generational equity topic, discussing perspectives for future generations. Both sections assess impacts from environmental, social and economic points of view.

Intra-generational equity aims at ensuring that all people from the present generation get the same access to resources, that costs and benefits from development are distributed evenly and that political and economic power are shared fairly.

From an environmental perspective, co-location including BESS enables an increased integration of renewable energy into the grid by mitigating challenges associated with the intermittency of sources like wind and solar through e.g. ancillary services or by storing surplus renewable energy during periods of low demand and supplying it during peak hours for energy arbitrage. Solar curtailment is a common issue as well, and PV-BESS colocation enables the storage of this excess energy. This globally leads to higher efficiency of the systems, being capable of harnessing more energy, and therefore maximizing renewable energy utilization. Despite these benefits, the BESS sector still has a non-negligible environmental impact on the present generation, mainly due to its manufacturing processes and the resources it needs. Batteries indeed use rare and disputed materials such as lithium and their extraction endangers ecosystems while being eager in other resources. For example, 1 ton of lithium requires 250 tons of ore, and the extraction process uses 1900 tons of water [66]. The manufacturing process is costly energy wise as well, as about 60kWh of energy is consumed to produce a 1kWh battery, emitting about 55 kg of carbon in the meantime [67].

The resource extraction and manufacturing of BESS also raises a social and ethical question, as some battery materials are sourced from countries with poor labor conditions, raising concerns about fair wages and environmental justice. Additionally, this resource extraction might not benefit those people directly, as batteries are mainly integrated in already large and interconnected grids in developed countries. However, when installed in remote places and connected to isolated micro-grids or simply weak grid areas, PV-BESS co-located systems help provide stable and cheaper energy supply and therefore enlarging energy access and electrification to remote rural areas. On the other hand, when built in dense electric grids, they help build a stronger infrastructure, more resilient to congestion, imbalance and extreme events. Overall costs for grid expansion are lowered as PV and BESS are installed. By allowing energy arbitrage, BESS also helps reduce wholesale market volatility, lowering electricity costs for consumers in the end. On the other hand, the reliance of BESS on trading in energy markets make its access limited to large energy companies operating on a grid scale. Therefore, the direct benefits from operations are concentrated in a few large companies.

Inter-generational equity aims at sharing evenly and fairly resources, costs and benefits of development with the future generation.

First, by enhancing renewable integration to the grid, BESS therefore helps accelerate the shift away from fossil fuels. On top of that, with its ability to take part in peak shaving operations, it lowers the need for fossil fuel-based power plants, often operating in those situations. Overall, BESS helps reduce carbon emissions of the energy sector and the dependence on fossil fuels for future generations. However, the use of Lithium nowadays and the large expansion of BESS will drastically impact the world lithium reserves, making this resource even more rare and disputed in the future. A way to tackle this problem is to build a large and stable recycling sector. However, the recycling of battery materials is still under development and cannot support the current need for batteries worldwide. The improvement of those processes will play an important role for the future of BESS and efforts are being made in that direction, e.g. the European Battery Alliance [8]. The lack of stable recycling sector will impact future generations in two ways: by making lithium extraction the only supply as mentioned, but also by creating a large waste source from all end-of-life batteries. Directly linked is a social issue of building today systems whose end of life will happen during the next generation. By developing such mid-term systems, the responsibility for their deconstruction and waste management is handed to the following generation. Nonetheless, BESS will still have positive benefits in the future. By helping to build strong and resilient grids, it provides long-term energy security, along with a shift out of fossil fuels volatile markets. In parallel, the deployment of BESS co-located with renewable will enhance investments in renewable energy sources.

8. Conclusion

This thesis has analyzed a methodology to size a battery system and assess the economic viability and operational implications of co-locating it with a PV power plant. A case study has been made for Hallstahammar, Sweden. The analysis considered two market participation strategies, arbitrage on the spot market and Frequency Containment Reserve for Disturbances (FCR-D) under three different grid connection scenarios.

The results indicate that arbitrage participation is not a financially viable option under the studied conditions. The Net Present Value (NPV) for all scenarios remains negative (over -3M€ in all 3 scenarios), with financial losses increasing as battery capacity grows. This is primarily due to the high operational costs (40.3k€/MW per year) exceeding potential revenues from arbitrage, despite Sweden's volatile electricity prices and their spread of about 50€/MWh, leading to average yearly earnings of 36.5k€/MW installed. Additionally, battery degradation from frequent charging and discharging cycles further contributes to financial losses. The only way to mitigate this loss was by utilizing excess PV power, which slightly improved the economic outcome but was insufficient to make arbitrage profitable.

On the other hand, FCR-D participation presents a significantly more promising economic case. Across all scenarios, FCR-D ensures stable revenues, resulting in positive NPVs up to 1.78M€ in Scenario 3. The optimal battery size under this strategy is notably higher, jumping respectively to 35MW and 41 MW in scenarios 1 and 2-3. The financial benefits of FCR-D come from a predictable revenue stream, primarily from the Up market, which offers higher prices compared to the Down market. The inclusion of excess PV power in Scenario 3 further increased total revenue by about 1M€, confirming the value of integrating renewable energy storage with ancillary services.

From a technical perspective, battery degradation was more pronounced in arbitrage due to frequent full charging and discharging cycles, leading to higher capacity loss over the project's lifetime (36% over 15 years). In contrast, FCR-D operation induced lower degradation (between 11.4 and 11.9%), primarily driven by calendar aging rather than deep cycling, making it a more sustainable option for long-term battery operation.

Overall, this study highlights the critical importance of market selection in determining the financial feasibility of energy storage co-located with PV. While arbitrage under current market conditions is not viable, participation in FCR-D offers a strong business case, supporting Sweden's transition toward a renewable-powered electricity grid. Future work could explore the impact of regulatory changes, dynamic market pricing, and technological advancements in battery storage to further optimize co-location strategies.

9. References

- [1] “The European Green Deal - European Commission,” July 14, 2021. https://commission.europa.eu/strategy-and-policy/priorities-2019-2024/european-green-deal_en.
- [2] International Energy Agency (IEA), “Technology Roadmap Energy Storage,” 2014.
- [3] International Renewable Energy Agency (IRENA), “FUTURE OF SOLAR PHOTOVOLTAIC Deployment, investment, technology, grid integration and socio-economic aspects”, 2019
- [4] International Energy Agency (IEA), Birol, Dr Fatih. “Batteries and Secure Energy Transitions,” n.d.
- [5] “Global Energy Storage and Grids Pledge.” . <https://cop29.az/en/pages/global-energy-storage-and-grids-pledge-background-information>.
- [6] BloombergNEF. “Lithium-Ion Battery Pack Prices See Largest Drop Since 2017, Falling to \$115 per Kilowatt-Hour: BloombergNEF,” December 10, 2024. <https://about.bnef.com/blog/lithium-ion-battery-pack-prices-see-largest-drop-since-2017-falling-to-115-per-kilowatt-hour-bloombergnef/>.
- [7] “Analysts Are Looking Forward to a Terawatt-Hour Battery Market.” <https://www.pacificgreen.com/articles/analysts-are-looking-forward-terawatt-hour-battery-market/>.
- [8] European Battery Alliance. “Building a European Battery Industry.” <https://www.eba250.com/>.
- [9] Raw Materials Information System (RMIS) “RMIS - Lithium-Based Batteries Supply Chain Challenges.” <https://rmis.jrc.ec.europa.eu/analysis-of-supply-chain-challenges-49b749>.
- [10] Diouf, Boucar, and Ramchandra Pode. “Potential of Lithium-Ion Batteries in Renewable Energy.” *Renewable Energy* 76 (April 2015): 375–80. <https://doi.org/10.1016/j.renene.2014.11.058>.
- [11] World Economic Forum. “Reliance on Renewable Generation Alone Is an Incomplete Solution for Grid-Supplied #energy. Here’s Why — and What We Should Do about It.,” August 30, 2023. <https://www.weforum.org/stories/2023/08/storage-is-the-key-to-the-renewable-energy-revolution/>.
- [12] Pusceddu, Elian, Behnam Zakeri, and Giorgio Castagneto Gissey. “Synergies between Energy Arbitrage and Fast Frequency Response for Battery Energy Storage Systems.” *Applied Energy* 283 (February 2021): 116274. <https://doi.org/10.1016/j.apenergy.2020.116274>.
- [13] D. Zafirakis, K. J. Chalvatzis, G. Baiocchi, and G. Daskalakis, “The value of arbitrage for energy storage: Evidence from European electricity markets,” *Applied Energy*, vol. 184, pp. 971–986, Dec. 2016, doi: [10.1016/j.apenergy.2016.05.047](https://doi.org/10.1016/j.apenergy.2016.05.047).
- [14] J. Villar, R. Bessa, and M. Matos, “Flexibility products and markets: Literature review,” *Electric Power Systems Research*, vol. 154, pp. 329–340, Jan. 2018, doi: [10.1016/j.epsr.2017.09.005](https://doi.org/10.1016/j.epsr.2017.09.005).
- [15] C. A. Murphy, A. Schleifer, and K. Eurek, “A taxonomy of systems that combine utility-scale renewable energy and energy storage technologies,” *Renewable and Sustainable Energy Reviews*, vol. 139, p. 110711, Apr. 2021, doi: [10.1016/j.rser.2021.110711](https://doi.org/10.1016/j.rser.2021.110711).
- [16] S. Nojavan, M. Majidi, and N. N. Esfetanaj, “An efficient cost-reliability optimization model for optimal siting and sizing of energy storage system in a microgrid in the presence of responsible load management,” *Energy*, vol. 139, pp. 89–97, Nov. 2017, doi: [10.1016/j.energy.2017.07.148](https://doi.org/10.1016/j.energy.2017.07.148).

- [17] R. Gupta, M. C. Soini, M. K. Patel, and D. Parra, "Levelized cost of solar photovoltaics and wind supported by storage technologies to supply firm electricity," *Journal of Energy Storage*, vol. 27, p. 101027, Feb. 2020, doi: [10.1016/j.est.2019.101027](https://doi.org/10.1016/j.est.2019.101027).
- [18] X. Han, J. Garrison, and G. Hug, "Techno-economic analysis of PV-battery systems in Switzerland," *Renewable and Sustainable Energy Reviews*, vol. 158, p. 112028, Apr. 2022, doi: [10.1016/j.rser.2021.112028](https://doi.org/10.1016/j.rser.2021.112028).
- [19] Y. Rivera-Durán, C. Berna-Escriche, Y. Córdova-Chávez, and J. L. Muñoz-Cobo, "Assessment of a Fully Renewable Generation System with Storage to Cost-Effectively Cover the Electricity Demand of Standalone Grids: The Case of the Canary Archipelago by 2040," *Machines*, vol. 11, no. 1, p. 101, Jan. 2023, doi: [10.3390/machines11010101](https://doi.org/10.3390/machines11010101).
- [20] R. Zhu, K. Das, P. E. Sørensen, and A. D. Hansen, "Optimal Participation of Co-Located Wind–Battery Plants in Sequential Electricity Markets," *Energies*, vol. 16, no. 15, p. 5597, Jul. 2023, doi: [10.3390/en16155597](https://doi.org/10.3390/en16155597).
- [21] J. A. Tejero-Gómez and Á. A. Bayod-Rújula, "Analysis of Photovoltaic Plants with Battery Energy Storage Systems (PV-BESS) for Monthly Constant Power Operation," *Energies*, vol. 16, no. 13, Art. no. 13, Jan. 2023, doi: [10.3390/en16134909](https://doi.org/10.3390/en16134909).
- [22] K. Vaillancourt, O. Bahn, E. Frenette, and O. Sigvaldason, "Exploring deep decarbonization pathways to 2050 for Canada using an optimization energy model framework," *Applied Energy*, vol. 195, pp. 774–785, Jun. 2017, doi: [10.1016/j.apenergy.2017.03.104](https://doi.org/10.1016/j.apenergy.2017.03.104).
- [23] A. S. Aziz, M. F. N. Tajuddin, T. E. K. Zidane, C.-L. Su, A. J. K. Alrubaie, and M. J. Alwazzan, "Techno-economic and environmental evaluation of PV/diesel/battery hybrid energy system using improved dispatch strategy," *Energy Reports*, vol. 8, pp. 6794–6814, Nov. 2022, doi: [10.1016/j.egy.2022.05.021](https://doi.org/10.1016/j.egy.2022.05.021).
- [24] N. Blasutigh, S. Negri, A. Massi Pavan, and E. Tironi, "Optimal Sizing and Environmental-Economic Analysis of PV-BESS Systems for Jointly Acting Renewable Self-Consumers," *Energies*, vol. 16, no. 3, p. 1244, Jan. 2023, doi: [10.3390/en16031244](https://doi.org/10.3390/en16031244).
- [25] S. Korjani, F. Casu, A. Damiano, V. Pilloni, and A. Serpi, "An online energy management tool for sizing integrated PV-BESS systems for residential prosumers," *Applied Energy*, vol. 313, p. 118765, May 2022, doi: [10.1016/j.apenergy.2022.118765](https://doi.org/10.1016/j.apenergy.2022.118765).
- [26] Q. Hassan, B. Pawela, A. Hasan, and M. Jaszczur, "Optimization of Large-Scale Battery Storage Capacity in Conjunction with Photovoltaic Systems for Maximum Self-Sustainability," *Energies*, vol. 15, no. 10, p. 3845, May 2022, doi: [10.3390/en15103845](https://doi.org/10.3390/en15103845).
- [27] J.-T. Liao, Y.-S. Chuang, H.-T. Yang, and M.-S. Tsai, "BESS-Sizing Optimization for Solar PV System Integration in Distribution Grid," *IFAC-PapersOnLine*, vol. 51, no. 28, pp. 85–90, 2018, doi: [10.1016/j.ifacol.2018.11.682](https://doi.org/10.1016/j.ifacol.2018.11.682).
- [28] C. Abbey and G. Joos, "Supercapacitor Energy Storage for Wind Energy Applications," *IEEE Trans. on Ind. Applicat.*, vol. 43, no. 3, pp. 769–776, 2007, doi: [10.1109/TIA.2007.895768](https://doi.org/10.1109/TIA.2007.895768).
- [29] H. Rahmanifard and T. Plaksina, "Hybrid compressed air energy storage, wind and geothermal energy systems in Alberta: Feasibility simulation and economic assessment," *Renewable Energy*, vol. 143, pp. 453–470, Dec. 2019, doi: [10.1016/j.renene.2019.05.001](https://doi.org/10.1016/j.renene.2019.05.001).
- [30] Alam SMS, Mosier TM, Gevorgian V, Bennett B, Stark G. "Integrated hydropower and energy storage: current examples and future potential". U.S. Department of Energy; forthcoming.
- [31] J. Jorgenson, P. Denholm, and T. Mai, "Analyzing storage for wind integration in a transmission-constrained power system," *Applied Energy*, vol. 228, pp. 122–129, Oct. 2018, doi: [10.1016/j.apenergy.2018.06.046](https://doi.org/10.1016/j.apenergy.2018.06.046).

- [32] R. De Azevedo and O. Mohammed, "Profit-maximizing utility-scale hybrid wind-PV farm modeling and optimization," in *SoutheastCon 2015*, Fort Lauderdale, FL, USA: IEEE, Apr. 2015, pp. 1–8. doi: [10.1109/SECON.2015.7132892](https://doi.org/10.1109/SECON.2015.7132892).
- [33] A. S. O. Ogunjuyigbe, T. R. Ayodele, and O. A. Akinola, "Optimal allocation and sizing of PV/Wind/Split-diesel/Battery hybrid energy system for minimizing life cycle cost, carbon emission and dump energy of remote residential building," *Applied Energy*, vol. 171, pp.153–171, Jun. 2016, doi: [10.1016/j.apenergy.2016.03.051](https://doi.org/10.1016/j.apenergy.2016.03.051).
- [34] Interreg, "Release of the Optimal Sizing Calculator," Interreg CENTRAL EUROPE. [Online]. Available: <http://programme2014-20.interreg-central.eu/Content.Node/news/Realease-of-the-Optimal-Sizing-Calculator.html>
- [35] G. Xu, C. Shang, S. Fan, X. Zhang, and H. Cheng, "Sizing battery energy storage systems for industrial customers with photovoltaic power," *Energy Procedia*, vol. 158, pp. 4953–4958, Feb. 2019, doi: [10.1016/j.egypro.2019.01.693](https://doi.org/10.1016/j.egypro.2019.01.693).
- [36] X. Wu, R. Roychowdhury, H. Zhang, B. Feldman, and R. Smith, "Optimal BESS Sizing for PV Interconnection & Energy Arbitrage with Industrial Customers," in *2024 IEEE Power & Energy Society General Meeting (PESGM)*, Jul. 2024, pp. 1–5. doi: [10.1109/PESGM51994.2024.10688751](https://doi.org/10.1109/PESGM51994.2024.10688751).
- [37] M. T. Parry and T. Martinsen, "Multi-year analysis for optimal behind-the-meter battery storage sizing and scheduling: A Norwegian case study," *Journal of Energy Storage*, vol. 110, p. 115304, Feb. 2025, doi: [10.1016/j.est.2025.115304](https://doi.org/10.1016/j.est.2025.115304).
- [38] M. A. Hannan, M. Faisal, P. Jern Ker, R. A. Begum, Z. Y. Dong, and C. Zhang, "Review of optimal methods and algorithms for sizing energy storage systems to achieve decarbonization in microgrid applications," *Renewable and Sustainable Energy Reviews*, vol. 131, p. 110022, Oct. 2020, doi: [10.1016/j.rser.2020.110022](https://doi.org/10.1016/j.rser.2020.110022).
- [39] M. Moghimi, R. Garmabdari, S. Stegen, and J. Lu, "Battery energy storage cost and capacity optimization for university research center," in *2018 IEEE/IAS 54th Industrial and Commercial Power Systems Technical Conference (I&CPS)*, Niagara Falls, ON: IEEE, May 2018, pp. 1–8. doi: [10.1109/ICPS.2018.8369968](https://doi.org/10.1109/ICPS.2018.8369968).
- [40] Serres C., "Evaluating the economic impact of lithium-ion battery degradation on grid-scale applications," *KTH*, 2024.
- [41] N. Mirzaei Alavijeh, *Flexibility from local resources: congestion management in distribution grids, carbon emission reductions and frequency containment reserves*. Göteborg: Chalmers University of Technology, 2024.
- [42] M. K. Nematchoua, J. A. Orosa, and M. Afaifia, "Prediction of daily global solar radiation and air temperature using six machine learning algorithms; a case of 27 European countries," *Ecological Informatics*, vol. 69, p. 101643, Jul. 2022, doi: [10.1016/j.ecoinf.2022.101643](https://doi.org/10.1016/j.ecoinf.2022.101643).
- [43] P. Bouquet, I. Jackson, M. Nick, and A. Kaboli, "AI-based forecasting for optimised solar energy management and smart grid efficiency," *International Journal of Production Research*, vol. 62, no. 13, pp. 4623–4644, Jul. 2024, doi: [10.1080/00207543.2023.2269565](https://doi.org/10.1080/00207543.2023.2269565).
- [44] S. C. Nwokolo, J. C. Ogbulezie, and O. J. Ushie, "A multi-model ensemble-based CMIP6 assessment of future solar radiation and PV potential under various climate warming scenarios," *Optik*, vol. 285, p. 170956, Aug. 2023, doi: [10.1016/j.ijleo.2023.170956](https://doi.org/10.1016/j.ijleo.2023.170956).
- [45] "CMIP Phase 6 (CMIP6) - Coupled Model Intercomparison Project." [Online]. Available: <https://wcrp-cmip.org/cmip6/>
- [46] T. Huld, E. Paietta, P. Zangheri, and I. Pinedo Pascua, "Assembling Typical Meteorological Year Data Sets for Building Energy Performance Using Reanalysis and Satellite-Based Data," *Atmosphere*, vol. 9, no. 2, p. 53, Feb. 2018, doi: [10.3390/atmos9020053](https://doi.org/10.3390/atmos9020053).

- [47] V. Munukutla, "Battery Optimization for Ancillary Markets in Nordic and Central European Electricity Markets," KTH, 2024.
- [48] S. Wilcox and W. Marion, "Users Manual for TMY3 Data Sets," Technical Report, 2008.
- [49] "Photovoltaic Geographical Information System (PVGIS) - European Commission." [Online]. Available: https://joint-research-centre.ec.europa.eu/photovoltaic-geographical-information-system-pvgis_en
- [50] I. Huber, L. Bugliaro, M. Ponater, H. Garny, C. Emde, and B. Mayer, "Do climate models project changes in solar resources?," *Solar Energy*, vol. 129, pp. 65–84, May 2016, doi: [10.1016/j.solener.2015.12.016](https://doi.org/10.1016/j.solener.2015.12.016).
- [51] CanadianSolar, "HiDM, High Density MONO PERC module 400W~420W", 2020.
- [52] Global Market Insights, "Europe Solar PV Module Market Size - By Technology (Thin Film, Crystalline Silicon), Product (Monocrystalline, Polycrystalline, Cadmium Telluride, Amorphous Silicon), Connectivity (On-Grid, Off-Grid), Mounting (Ground Mounted, Rooftop), 2025 – 2034," 2024
- [53] W. De Soto, S. A. Klein, and W. A. Beckman, "Improvement and validation of a model for photovoltaic array performance," *Solar Energy*, vol. 80, no. 1, pp. 78–88, Jan. 2006, doi: [10.1016/j.solener.2005.06.010](https://doi.org/10.1016/j.solener.2005.06.010).
- [54] K. S. Anderson, C. W. Hansen, W. F. Holmgren, A. R. Jensen, M. A. Mikofski, and A. Driesse, "pvlib python: 2023 project update," *JOSS*, vol. 8, no. 92, p. 5994, Dec. 2023, doi: [10.21105/joss.05994](https://doi.org/10.21105/joss.05994).
- [55] J. Nelson, *The Physics of solar cells*, Reprint 2007. Londres: Imperial College, 2007.
- [56] A. Driesse, P. Jain, and S. Harrison, "Beyond the curves: Modeling the electrical efficiency of photovoltaic inverters," in *2008 33rd IEEE Photovoltaic Specialists Conference*, San Diego, CA, USA: IEEE, May 2008, pp. 1–6. doi: [10.1109/PVSC.2008.4922827](https://doi.org/10.1109/PVSC.2008.4922827).
- [57] R. Kiesel, F. Paraschiv, and A. Sætherø, "On the construction of hourly price forward curves for electricity prices," *Comput Manag Sci*, vol. 16, no. 1–2, pp. 345–369, Feb. 2019, doi: [10.1007/s10287-018-0300-6](https://doi.org/10.1007/s10287-018-0300-6).
- [58] CATL "Storing Infinite Energy - CATL Products Brochure", [Online]. Available: https://www.catl.com/en/uploads/1/file/public/202406/20240624152558_gft6x51t14.pdf
- [59] kgi-admin, "Power plant profile: Hallstahammar Solar PV Park, Sweden," *Power Technology*. [Online]. Available: <https://www.power-technology.com/marketdata/power-plant-profile-hallstahammar-solar-pv-park-sweden/>
- [60] Flower Infrastructures Technology AB, [Online]. Available: <https://www.flower.se/>
- [61] A. R. Jensen *et al.*, "pvlib iotools—Open-source Python functions for seamless access to solar irradiance data," *Solar Energy*, vol. 266, p. 112092, Dec. 2023, doi: [10.1016/j.solener.2023.112092](https://doi.org/10.1016/j.solener.2023.112092).
- [62] Svenska Kraftnät, "Långsiktig marknadsanalys", 2024
- [63] Svenska Kraftnät, "Balancing market outlook 2030", 2024
- [64] Transparency Platform." [Online]. Available: <https://newtransparency.entsoe.eu/>
- [65] "Mimer | Svenska kraftnät." [Online]. Available: <https://mimer.svk.se/PrimaryRegulation/PrimaryRegulationIndex>
- [66] M. Terkes, Z. Öztürk, A. Demirci, and S. M. Tercan, "Optimal sizing and feasibility analysis of second-life battery energy storage systems for community microgrids considering carbon reduction," *Journal of Cleaner Production*, vol. 421, p. 138507, Oct. 2023, doi: [10.1016/j.jclepro.2023.138507](https://doi.org/10.1016/j.jclepro.2023.138507).
- [67] S. Davidsson Kurland, "Energy use for GWh-scale lithium-ion battery production," *Environ. Res. Commun.*, vol. 2, no. 1, p. 012001, Jan. 2020, doi: [10.1088/2515-7620/ab5e1e](https://doi.org/10.1088/2515-7620/ab5e1e).